Applied Geochemistry 118 (2020) 104608

Contents lists available at ScienceDirect

Applied Geochemistry

journal homepage: http://www.elsevier.com/locate/apgeochem

Geochemical mapping in stream sediments of the Carajás Mineral Province: Background values for the Itacaiúnas River watershed, Brazil

Gabriel Negreiros Salomão [a,b,1,*], Roberto Dall'Agnol [a,b], Prafulla K. Sahoo [b,c], Rômulo Simões Angélica [a], Carlos A. de Medeiros Filho [d], Jair da Silva Ferreira Júnior [b], Marcio Sousa da Silva [b,e], Pedro Walfir Martins e Souza Filho [a,b], Wilson da Rocha Nascimento Junior [b], Marlene F. da Costa [f], Luiz Roberto Guimarães Guilherme [g], José Oswaldo de Siqueira [b]

[a] Programa de Pós-graduação em Geologia e Geoquímica, Instituto de Geociências, Universidade Federal do Pará, Rua Augusto Corrêa, 1, Belém, 66075-110, PA, Brazil
[b] Instituto Tecnológico Vale, Rua Boaventura da Silva, 955, Belém, 66055-090, PA, Brazil
[c] Department of Environmental Science and Technology, School of Environmental and Earth Sciences, Central University of Punjab, Bathinda, 151001, India
[d] VALE S/A - Exploração Mineral. Rua Grajaú, 63, Carajás, Parauapebas, 68515-000, PA, Brazil
[e] Programa de Pós-graduação em Ciências Ambientais, Instituto de Geociências, Universidade Federal do Pará, Rua Augusto Corrêa, 1, Belém, 66075-110, PA, Brazil
[f] Gerência de Meio Ambiente - Minas de Carajás, Departamento de Ferrosos Norte, Estrada Raymundo Mascarenhas, S/N Mina de N4, 68516-000, Parauapebas, Pará, Brazil
[g] Departamento de Ciência do Solo, Universidade Federal de Lavras, Lavras, Minas Gerais, 37200-000, Brazil

ARTICLE INFO

Editorial handling by de Caritat Patrice

Keywords:
Multi-element analysis
Stream sediments
Microcatchment-based geochemical mapping
Iron
Potentially toxic elements
Southeastern amazon

ABSTRACT

Multi-elemental analysis of high-density (regional-scale) geochemical surveys is an important strategy for multi-purpose applications, particularly in addressing geochemical background concentrations in different sampling media. This approach was applied to the Itacaiúnas River Watershed (IRW), which is situated in the most prominent mining area of Brazil, the Carajás Mineral Province. Microcatchment-based mapping (~50 km^2 each) covering the whole extent of IRW was delimited using remote sensing techniques and targeted for sampling. A total of 788 samples, including 27 duplicates, were collected in 2017. The <0.177 mm fraction of all samples was digested by aqua regia and 51 elements were analyzed by inductively coupled plasma atomic emission spectroscopy (ICP-AES) and inductively coupled plasma mass spectrometry (ICP-MS). Geochemical maps for Fe and potentially toxic elements (PTE; As, Ba, Cd, Co, Cr, Cu, Hg, Mn, Mo, Ni, Pb, Sn, V, and Zn) and microcatchment-based distribution maps based on threshold values were constructed for the whole IRW. The stream sediment geochemistry is mainly controlled by the local geologic setting and underlying lithology. Geochemical background (GB) values for 43 elements in stream sediments of the IRW were determined by a variety of methods (Tukey's inner fences -TIF, median ± 2*median absolute deviation - MAD, and percentile-based techniques). The results provided from the different methods show a wide range of values, with the MAD method being considered the most appropriate for deriving GB concentrations. A comparison of reference levels for PTE contemplated in the Brazilian regulation in stream sediments, the threshold concentrations obtained for the IRW area, and different study cases around the world is presented in detail. Our findings provide not only valuable information for selecting potential areas for mineral exploration surveys, but also for evaluating geochemical contaminant effects with time-varying treatments. Studies conducted to determine background values at regional scale are needed for environmental decision making, as well as to attest actions in cases of potential contamination. In the absence of these studies, misleading interpretations of the magnitude of contamination levels in a certain area may cause under- or overestimation of ecological and/or human-health risks of PTE.

* Corresponding author. Universidade Federal do Pará, Instituto de Geociências, Programa de Pós-Graduação Geologia e Geoquímica, Rua Augusto Corrêa, 01. Guamá, 66075-110, Belém – Pará, Brazil.
E-mail address: salomao.gn@gmail.com (G.N. Salomão).
[1] Present address: Rua Augusto Corrêa, 01. Guamá. 66075-110. Belém – Pará, Brazil. Universidade Federal do Pará, Instituto de Geociências, Programa de Pós-Graduação Geologia e Geoquímica.

https://doi.org/10.1016/j.apgeochem.2020.104608
Received 31 October 2019; Received in revised form 14 December 2019; Accepted 19 April 2020
Available online 18 May 2020

1. Introduction

Exploration and environmental geochemistry are research areas that rely strongly on geochemical background (GB). The concept of GB has not been clearly established and many different definitions of the term have been used in the literature (Matschullat et al., 2000; Reimann et al., 2018, 2005; Reimann and Garrett, 2005). Essentially, GB is often used to distinguish between natural and anthropogenic element concentrations (Reimann and Caritat, 2005). The upper background limit (UBL, also known as threshold) is regularly used as reference to define action levels in environmental legislation (Reimann et al., 2018; Reimann and Caritat, 2017). On the other hand, the lower background limit (LBL) has not been widely discussed, perhaps due to its low relevance for exploration purposes. However, the Water Quality Guidelines (WQGs) protocol of Australia and New Zealand (Australian and New Zealand Environment and Conservation Council - ANZECC and Agriculture and Resource Management Council of Australia and New Zealand - ARMCANZ, 2000) suggest not only the calculation of threshold values (UBL), but also of LBLs as an important starting point to derive guideline values for stressor and ecosystem receptor components, particularly for potentially toxic elements (PTE). For instance, ANZECC and ARMCANZ (Australian and New Zealand Environment and Conservation Council - ANZECC and Agriculture and Resource Management Council of Australia and New Zealand - ARMCANZ, 2000) suggest the use of the 80th percentile of reference-site data to derive threshold, and the 20th percentile for stressors that could cause problems at low concentrations. More conservative guideline values have been applied as a precautionary measure where there are indications that deviation from the ideal reference condition has potential to adversely affect ecosystems (Ander et al., 2013; Australian and New Zealand Environment and Conservation Council - ANZECC and Agriculture and Resource Management Council of Australia and New Zealand - ARMCANZ, 2000).

Multi-elemental analysis of high-density geochemical surveys (MEA-HDGS) is an important strategy in addressing GB levels for multi-purpose applications (Caritat and Cooper, 2016; Cheng et al., 2014; Costa et al., 2015; Labuschagne et al., 1993; Ripin et al., 2014; Salminen and Tarvainen, 1997; Yuan et al., 2013). MEA-HDGS can provide detailed information about the spatial variability of chemical elements in relation to different influencing factors (e.g., geological domains, topography, mineralization zones) in multiple sampling medias (e.g., soils, water and sediments) (Ander et al., 2013; Reimann et al., 2018). Under these circumstances, stream sediments collected at the catchment outlet are representative of the source catchment area, and can provide important information to evaluate the role of geogenic and/or anthropogenic sources of contribution (Albanese et al., 2007; Darnley and Garrett, 1990; Darnley et al., 1995; Gałuszka, 2007; Plant et al., 2001).

In Brazil, GB studies of stream sediment data from MEA-HDGS are scarce, particularly in the Amazon region. The present study is associated to the 'Itacaiúnas Geochemical Mapping and Background Project' (ItacGMBP), a regional scale MEA-HDGS being executed by the Instituto Tecnológico Vale (ITV) in the Itacaiúnas River watershed (IRW, Fig. 1). The IRW (~42,000 km^2) is located in the north of the Tocantins Basin, Brazil (Fig. 1). The region has ~700,000 inhabitants and encompasses four major urban areas. It has a tropical monsoon climate (Alvares et al., 2013) and was originally covered by the Amazon rainforest (Souza-Filho et al., 2016). The topography of the region is divided into the Carajás plateau (400–900 m), where most of the protected environmental areas covered by pristine tropical forest are situated, and adjacent lower lands (80–300 m) with predominance of pasturelands (Fig. 1). The IRW is particularly relevant for geochemical studies because it is located in the Carajás Mineral Province, the largest mining district of Brazil with active mines of iron, copper, nickel, and manganese. Previous geochemical surveys have been conducted in the region by the Geological Survey of Brazil (Companhia de Pesquisa de Recursos Minerais - CPRM, 2013; 2012) and studies covering parts of the IRW have been recently published (Salomão et al., 2018, 2019b, 2019a).

This study aims to present the results of geochemical mapping and estimate GB values for 51 elements in stream sediment geochemical data of the IRW using a series of statistical tools and geospatial techniques (Cave et al., 2012; Johnson et al., 2012; Matschullat et al., 2000; Reimann et al., 2018). Distribution maps based on threshold values were created for the main elements related to mining in the province and for PTE contemplated in the Brazilian environmental regulation (Conselho Nacional de Meio Ambiente - CONAMA, 2012). Threshold values are compared with stream sediment quality guideline values and their significance as possible protective values is discussed. This study provides geochemical reference values for stream sediments in an extremely important mining province in the Amazon region.

2. Geological setting

The IRW exhibits a complex geological setting located in an area

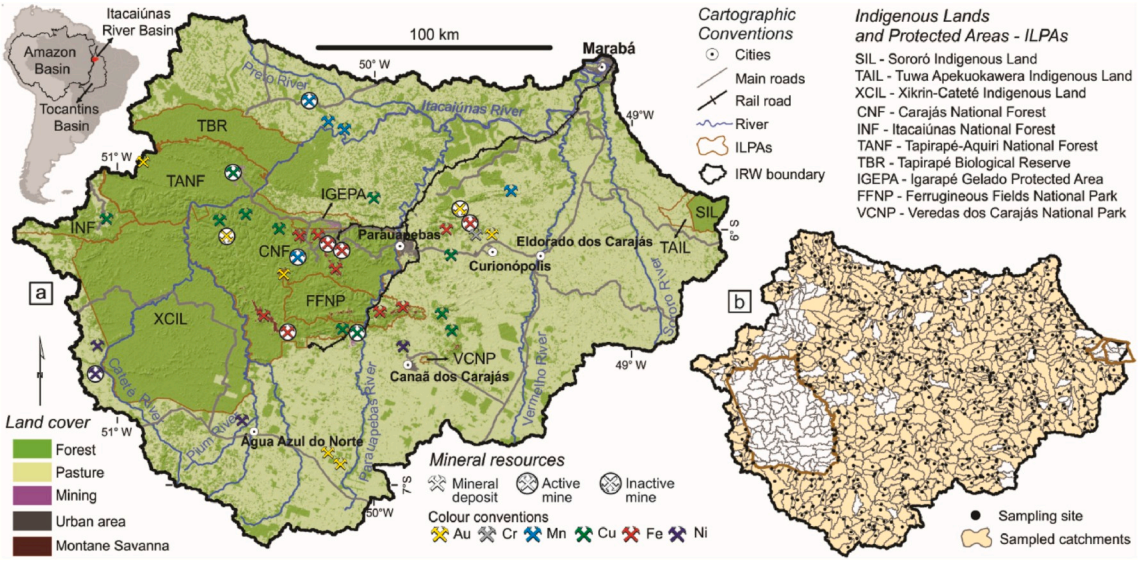

Fig. 1. Location of the study area in the southeast of the State of Pará, Brazil, showing: a land cover and land use map of the Itacaiúnas River watershed in 2013 (Souza-Filho et al., 2016) with the location of main cities and towns, mines, indigenous lands and environmental protected areas - ILPAs (a); Distribution of catchments and location of sediment samples for the ItacGMBP project (b).

comprising the eastern Amazonian Craton and the extreme north of the Araguaia Belt (Fig. 2a) (Alkmim, 2015; Feio et al., 2013; Martins et al., 2017; Santos, 2003). For the purpose of geochemical mapping, the study area can be divided into four main geologic settings (Dall'Agnol et al., 2013; Feio and Dall'Agnol, 2012; Santos et al., 2013): Rio Maria, Sapucaia and Canaã dos Carajás domains (RM-S-CC), that occupy the southern portion of the IRW; Carajás Basin (CB), in its central portion; Bacajá Domain (BD), to the north; and Araguaia belt (AB), to the east (Fig. 2).

The RM-S-CC domains are formed mainly by Mesoarchean granitoids, with composition ranging from tonalite-trondhjemite-granodiorite (TTG), Mg-rich granitoids (sanukitoids) and leucogranodiorites to leucogranites, as well as granulitic units (Chicrin-Cateté Orthogranulite), and metamafic-ultramafic greenstone belts (Feio et al., 2013; Machado et al., 1991; Moreto et al., 2015). During the Neoarchean were formed A-type granitoids, charnockitic and mafic-ultramafic bodies that cross-cut Mesoarchean units (Barros et al., 2009; Dall'Agnol et al., 2017; Mansur and Ferreira Filho, 2017; Marangoanha et al., 2019; Rosa, 2014). In the RM-S-CC domains are located the Onça-Puma (Ni) and Sossego (Cu) active mines.

The CB is composed of Neoarchean metavolcano-sedimentary sequences with dominance of mafic to intermediate rocks and banded iron formations (BIF), the latter responsible for the Fe deposits of the Carajás region (Gibbs et al., 1986; Machado et al., 1991; Martins et al., 2017). These sequences are cross-cut by Neoarchean A-type granite plutons (Barros et al., 2009; Sardinha et al., 2006), and minor mafic–ultramafic stratified bodies (Vasquez et al., 2008), and by Paleoproterozoic A-type granite suites. Important Fe (N4, N5, S11D and Serra Leste) and Mn (Azul) mines are located in this segment.

In the BD, the most widely distributed rocks are high-grade charnockite rocks from the Cajazeiras Complex, with subordinate mafic ortho-granulite and metasedimentary high-grade rocks, supracrustal metamorphic rocks (greenschist to amphibolite facies) of the Tapirapé Formation, and metasedimentary lithologies of the Buritirama Formation, with associated ultramafic schists and BIFs (Macambira et al., 2009; Vasquez et al., 2008; and references therein). In this domain is located the Buritirama mine (Mn).

The AB is mainly composed of low grade metasedimentary rocks of the Couto Magalhães and Pequizeiro formations (Alvarenga et al., 2000). Associated to those units, there occur some mafic-ultramafic bodies (Vasquez et al., 2008). Sedimentary units of the Phanerozoic Parnaíba Basin cover locally the units of the AB and BD (Vasquez et al., 2008). Quaternary lateritic crusts and alluvial deposits have greater expression in the AB (Vasquez et al., 2008).

3. Material and methods

3.1. The computer-based framework for the high density geochemical survey

A computer-based framework associated with Geographic Information System (GIS) was set up to provide support in sampling strategies, data storage, screening and validation. A specific geochemical database was structured to guide sample location and store all field data using tablets and gradually additional related information as analytical results and geochemical maps. The structure of the framework is essentially composed of three integrated components (Fig. 3):

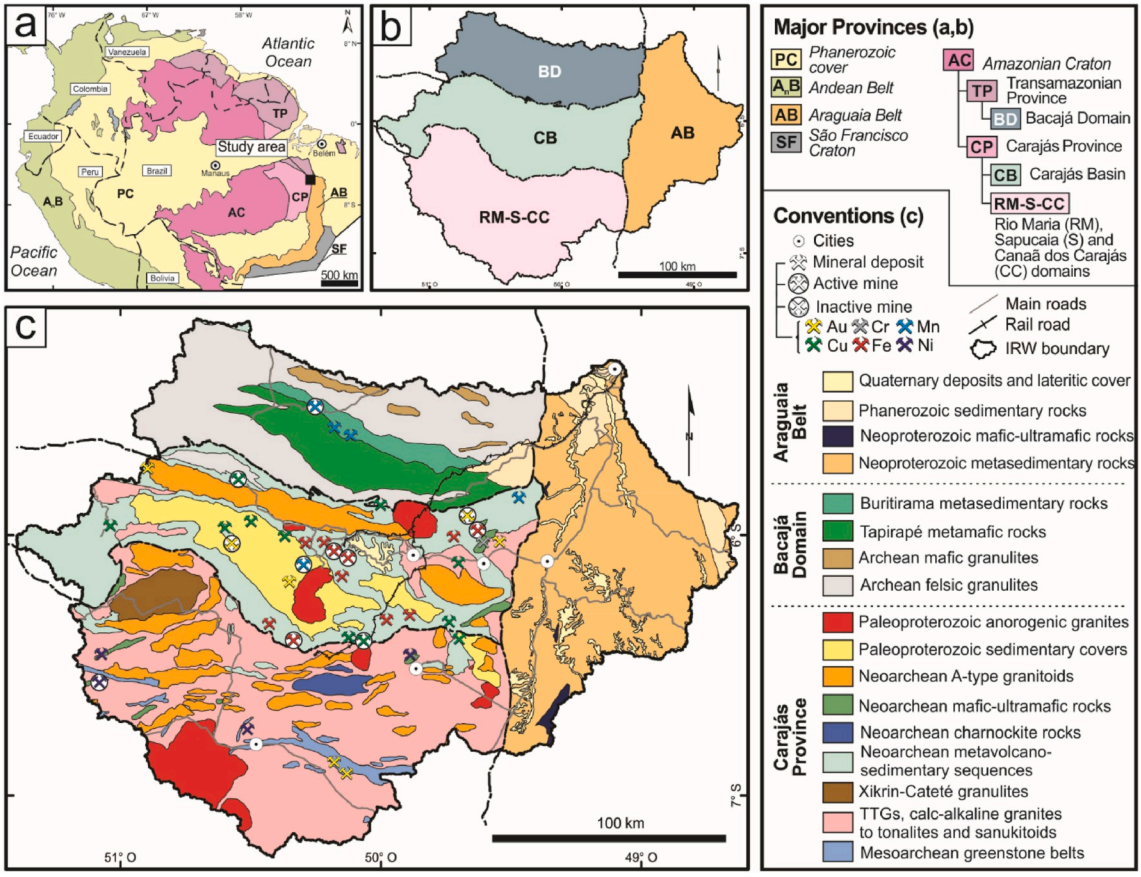

Fig. 2. Geological setting. a) Amazonian Craton, showing the Transamazonian and Carajás provinces, and Araguaia belt (Santos et al., 2000; simplified). b) Simplified geological domains in the Itacaiúnas river watershed. c) Simplified geological map of the Itacaiúnas river watershed (Vasquez et al., 2008, modified; and references therein). Figure based on Sahoo et al. (2019b).

i. An iPad application for sample collection developed in Swift, which allows a real time connectivity among field work teams and the operational office.
ii. A server back-end written in Java, which receives data from iPads in the field, and acts as a central repository for sample data sharing, by using a combination of scripts developed in R (R Core Team, 2013) and QGIS (QGIS Development Team, 2009).
iii. R scripts generate reports and statistical plots, match analysis data from the laboratory with their corresponding samples in the database, and detect anomalous results due to laboratory error.

3.2. Sampling strategy

Initially 920 microcatchments (~50 km^2 each) covering the whole extent of IRW were delimited using remote sensing techniques and targeted for sampling. As a rule, only one representative sample should be collected near the outlet of the respective microcatchment, but this was impossible in some places due to limited access. The final distribution of the sampled catchments is shown in Fig. 1. After strong efforts to access a maximum of sampling sites, 761 catchments could be sampled and, of these, 27 were sampled in duplicate. Most of the unsampled sites are located in indigenous lands and remote protected areas covered by tropical forest with severe access limitations. For each sampling site, two samples, one of stream water and another of stream sediment were collected. Stream water sampling procedure and geochemical results are presented by Sahoo et al. (2019) and Salomão et al. (2018). Sediment samples (3 kg per sample) were collected from 0 to 10 cm depth.

3.3. Sample preparation and chemical analyses

All samples were oven-dried at 70 °C and homogenized and a bulk split (c. 50%) of each sample was archived for future investigations. The remainder material was riffle split and sieved to <80 mesh (0.177 mm) fraction. Approximately 50 g of stream sediment samples was grounded and sieved through a 200 mesh (<75 μm) sieve and stored in polythene bags. Microwave assisted, aqua regia (HNO_3 + 3HCl) digestion of the <75 μm fraction produced the analyte for chemical analyses. Chemical analyses were carried out for 51 elements using Inductively Coupled Plasma - Atomic Emission Spectrometry (ICP-AES; Al, Ca, Fe, K, Mg, Na, S, and Ti), and Inductively Coupled Plasma - Mass Spectrometry (ICP-MS; Ag, As, Au, B, Ba, Be, Bi, Cd, Ce, Co, Cr, Cs, Cu, Ga, Ge, Hf, Hg, In, La, Li, Mn, Mo, Nb, Ni, P, Pb, Rb, Re, Sb, Sc, Se, Sn, Sr, Ta, Te, Th, Tl, U, V, W, Y, Zn, and Zr) at ALS Brasil Ltda, a certified/accredited laboratory. Six certified reference materials (AMIS0096, BCS-348, BXMG-5, GBM303-4, GBM908-10 and MRGeo08) were used for quality assurance and quality control (QA/QC) purposes. Protocols for sample preparation and analytical methods are similar to those adopted by the National Geochemical Survey of Australia (NGSA) manuals (Caritat et al., 2009).

3.4. Statistical data analysis for the determination of geochemical background values

The whole dataset of stream sediments chemical analyses was submitted to non-parametric statistics and exploratory data analysis. Censored data (analytical values below the detection limit, <LLD) were replaced by ½LLD. Descriptive statistical parameters and normality (Lilliefors test) of element concentrations were calculated. In addition, to the results of univariate statistics (e.g., boxplots, histograms and probability plots) simple common logarithmic (log_{10}) transformation was applied, whenever appropriate. Data analysis was performed under R programming language in RStudio (RStudio Team, 2015), associated to a combination of R packages (Epskamp et al., 2018; Filzmoser, 2015; Gross and Ligges, 2015).

Geochemical background values were determined integrating a variety of statistical methods: the Tukey's inner fences (TIF), the median ± 2*median absolute deviation (MAD), the 98th, 95th, 90th and 75th percentiles (Ander et al., 2013; Cembranel et al., 2017; Reimann et al., 2018, 2005; Reimann and Caritat, 2017, 2005; Salomão et al., 2018).

A requirement for using TIF and MAD techniques is that for a given dataset, the element should follow a normal distribution (Reimann et al., 2018, 2008), unusually seen in geochemical dataset. Hence, to use those methods, the data should be prior transformed to common logarithm (log_{10}) scale (Eq. (1)), where $x_{(i,j)}$ is the raw dataset (usually in mg kg^{-1} or/and at.%) and $y_{(i,j)}$ is the log_{10} transformed data. Then the results are back-transformed by raising 10 to the power of the obtained result.

$$y_{(i,j)} = \log_{10}\left[x_{(i,j)}\right] \quad (1)$$

The TIF method was originally based on Tukey (1977) and it is strongly recommended by Matschullat et al. (2000) and Reimann et al. (2005). The upper (Q3) and lower (Q1) quartiles (often referred as hinges) of the boxplot, contains approximately 50% of the data. Then, the inner fence is determined as the interquartile range (IQR) extended by 1.5 times, and the upper and the lower whiskers are defined as the farthest observation inside the inner fence from each end of the box. The UBL or threshold value and the LBL based on TIF method are calculated following Eq. (2) and Eq. (3), respectively:

$$TIF_{Upper\ limit} = 10^{\left(Q_{3(y)} + 1.5 \cdot IQR_{(y)}\right)} \quad (2)$$

$$TIF_{Lower\ limit} = 10^{\left(Q_{1(y)} - 1.5 \cdot IQR_{(y)}\right)} \quad (3)$$

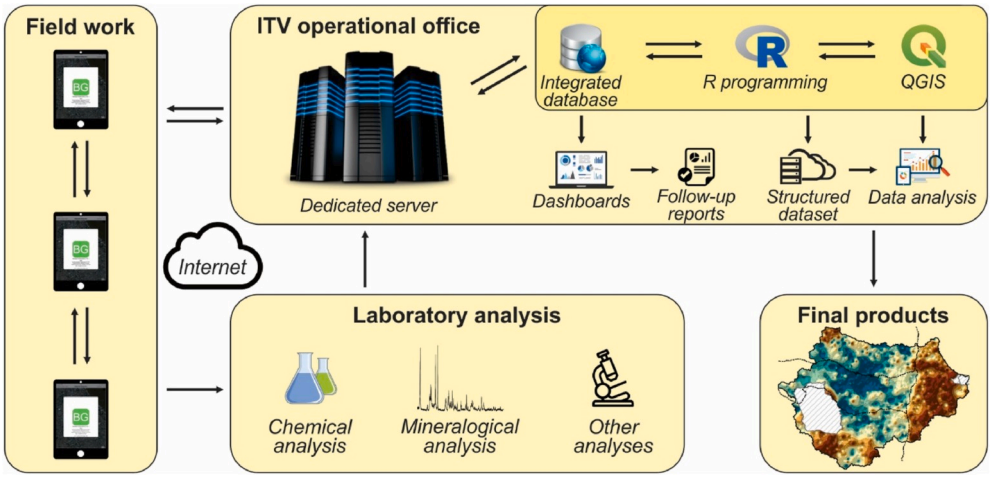

Fig. 3. Schematic representation of the computer-based framework for the ItacGMBP project development.

According to Reimann et al. (2018), the TIF method depends only on the data distribution and it allows the definition of background values even if no outliers are present in the data set. In other words, the obtained UBL can be greater than the maximum value obtained in the dataset, as it extrapolates from the Q1 to Q3 quartiles of the data's structure. However, the boxplot function is most informative if the true number of outliers is below 10% (Reimann et al., 2005).

The MAD is one of the most prestigious methods for deriving background values (Reimann et al., 2005). In this approach, the median absolute deviation (MAD_j, Eq. (4)), calculated with a constant of 1.48, leads to a consistent estimation of the underlying standard deviation (Reimann et al., 2018).

$$MAD_{(y)} = 1.48 \cdot median_i \left| y_i - median_j (y_j) \right| \quad (4)$$

At this stage, the result should be back-transformed according to Eq. (5) and Eq. (6) in order to derive the UBL and LBL, respectively:

$$MAD_{Upper\ limit} = 10^{\left(median_{(y)} + 2 \cdot [MAD_y]\right)} \quad (5)$$

$$MAD_{Lower\ limit} = 10^{\left(median_{(y)} - 2 \cdot [MAD_y]\right)} \quad (6)$$

The most simplistic methods for deriving UBL or threshold values are the percentile-based approaches (Ander et al., 2013). The 98th percentile presents similar results to the Mean + 2*SD, when a normal distribution of a given element is satisfied (Hawkes and Webb, 1962; Reimann et al., 2005; and references therein). The 95th percentile corresponds to a more restricted background range, so it considers the 5% of all samples as upper 'outliers'. For the present study the 90th and 75th percentiles were considered because they were suggested as a possible quality guidelines by CONAMA (2012, 2009, 2004). The adopted LBLs follow the proportionally for the left side of the distribution (e.g., 2%–98%; 5%–95%; 10%–90%; 25%–75%, cf. Fig. 4).

Geochemical background results were compared in cumulative probability (CP) distribution diagrams (Ander et al., 2013; Cave et al., 2012; Johnson et al., 2012) and are presented for selected elements in the result section and for all 51 elements in supplementary materials (Fig. 8SM). CP diagrams are considered the most rigorous procedure for the establishment of background values (Reimann et al., 2018). However, this method did not receive the preference of the present authors because it involves a certain amount of subjectivity.

3.5. Spatial representation of stream sediment geochemical data

The GIS environment was designed according to the World Geodetic System 1984 (WGS84) datum. The software ArcGIS 10.4.1 (Esri, 2016) was used for the construction of maps and for geospatial techniques. Spatial distribution maps of stream sediments were based on two techniques: i) spatial interpolation according to the classic Inverse Distance Weighting (IDW) method (Cheng et al., 2014; Lima et al., 2003) for the evaluation of regional geochemical patterns; and, ii) Catchment-based representation of uni-element concentrations in stream sediment (Bonham-Carter et al., 1987; Carranza, 2011; Carranza and Hale, 1997; Salomão et al., 2018) based on threshold values for the identification of concentrations above the regional background.

4. Results

The integrated results for the stream sediment geochemical data of the ItacGMBP project are presented here for the first time. Descriptive statistics of the 51 analyzed chemical elements in 761 samples are summarized in Table 1 in both, raw and log_{10}-transformed data. The lower (LLD) and upper (ULD) limits of detection for the analytical method adopted in the project, as well as their concentration units, are also presented (Table 1). The proportion of analytical values < LLD revealed that the large majority of the elements (40) has <15% of data < LLD; Sb, Na, Te, Ge, S, and Se have 20–62% of data < LLD; and, Au, Ta, Re, B, and W have >80% of data < LLD. No analytical values exceeded the ULD. The mean, minimum, 1st quartile (Q1), median (M), 3rd quartile (Q3), maximum concentration and measures of variation/deviation (e.g., standard deviation, median absolute deviation, skewness and kurtosis) are presented in Table 1. Normality test revealed non normal distribution (p value < 0.001) for all elements in raw data. Log_{10}-transformed data of some elements (e.g., Pb, Ga, La, Sr, P, U, Th, Co, Y, V, Al, Mn, Rb) follows a normal distribution or get closer to it. To complement the descriptive statistics, a comparison of boxplots ordered by increasing median in mg kg^{-1} converted to log10 transformed data is displayed in Fig. 5.

In this study, spatial distribution maps were constructed only for Fe and PTE. IDW interpolation maps for Fe, Mn, Cr, Ni, Cu, Mo, As, and Hg (Fig. 6) and Ba, Cd, Co, Pb, Sn, V, and Zn (Fig. 6SM) were constructed to evaluate their regional distribution. Catchment-based distribution maps based on threshold values for As, Cd, Cr, Cu, Hg, Ni, Pb, and Zn (Fig. 7) and Fe, Mn, Ba, Co, Mo, Sn, and V (Fig. 7SM) were used to identify concentrations above the regional background (cf. Table 2).

Geochemical background values for 43 elements in 761 stream sediment sites of the IRW estimated by a variety of methods (TIF, MAD, and percentile-based background) and the number of samples <LBL and >UBL are presented in Table 2SM. Eight elements, Au, B, Ge, Re, S, Sb, Ta, and Te were not included in Table 2SM because they presented a large proportion of values < LLD. In this study, only threshold values of Fe and selected PTE (As, Ba, Cd, Co, Cr, Cu, Hg, Mn, Mo, Ni, Pb, Sn, V, and Zn) are going to be discussed (Table 2). CP distribution plots were

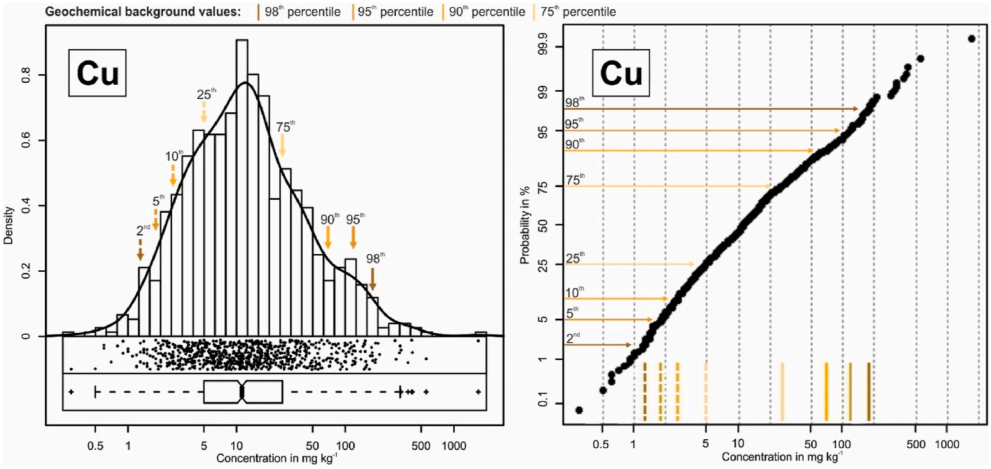

Fig. 4. Percentile-based approaches for deriving geochemical background.

Table 1
Statistical summary of aqua regia soluble concentration measured by ICP-AES and ICP-MS of 14 selected PTE and Fe in 761 active stream sediment samples of the IRW. Table 1SM in Supplementary material has information for all 51 elements.

Elements	Unit	LLD - ULD	<LLD (%)	Mean		SD		MAD		SKEW		Rku		min		Q1		M		Q3		max		p.Lt	
				RD	Log_{10}	RD	Log_{10}	RD	Log_{10}	RD	Log_{10}	RD	Log_{10}	RD	Log_{10}	RD	Log_{10}	RD	Log_{10}	RD	Log_{10}	RD	Log_{10}	RD	Log_{10}
As	mg kg^{-1}	0.1–10,000	4.7	1.60	−0.24	3.06	0.60	1.39	0.88	5.07	0.40	44.27	−0.46	<0.1	−1.30	0.20	−0.70	0.50	−0.30	1.50	0.18	41.80	1.62	<0.001	<0.001
Ba	mg kg^{-1}	10 - 10,000	0.1	78.38	1.77	73.10	0.32	148.96	2.30	4.78	−0.16	38.19	0.57	<10	0.70	40.00	1.60	60.00	1.78	90.00	1.95	900.00	2.95	<0.001	<0.001
Cd	mg kg^{-1}	0.01–1000	14.0	0.02	−1.82	0.04	0.35	0.02	−1.11	6.5	0.93	58.24	1.09	<0.01	−2.30	0.01	−2.00	0.01	−2.00	0.02	−1.70	0.46	−0.34	<0.001	<0.001
Co	mg kg^{-1}	0.1–10,000	0.0	8.97	0.72	10.93	0.45	14.49	1.64	3.05	0.10	12.95	−0.43	0.30	−0.52	2.50	0.40	5.00	0.70	10.80	1.03	97.50	1.99	<0.001	0.037
Cr	mg kg^{-1}	1 - 10,000	0.0	46.16	1.40	114.29	0.43	65.51	2.19	16.29	0.38	346.56	0.60	2.00	0.30	13.00	1.11	24.00	1.38	47.00	1.67	2630.00	3.42	<0.001	<0.001
Cu	mg kg^{-1}	0.2–10,000	0.0	30.05	1.08	78.85	0.55	33.74	2.14	13.32	0.36	254.85	0.11	0.30	−0.52	5.00	0.70	11.20	1.05	26.40	1.42	1680.00	3.23	<0.001	<0.001
Fe	at.%	0.01–50	0.0	2.96	4.31	3.41	0.36	4.72	5.03	4.11	0.38	25.18	−0.07	0.28	3.45	1.08	4.03	1.87	4.27	3.55	4.55	35.40	5.55	<0.001	<0.001
Hg	mg kg^{-1}	0.01–10,000	4.4	0.04	−1.59	0.03	0.36	0.09	−0.87	2.35	0.11	7.95	−0.56	<0.01	−2.30	0.01	−2.00	0.03	−1.52	0.05	−1.30	0.27	−0.57	<0.001	<0.001
Mn	mg kg^{-1}	5 - 50,000	0.0	715.67	2.61	1100.18	0.45	1204.74	3.58	5.83	0.17	46.44	−0.12	25.00	1.40	188.00	2.27	416.00	2.62	837.00	2.92	12,000.00	4.08	<0.001	0.008
Mo	mg kg^{-1}	0.05–10,000	0.0	0.44	−0.52	0.78	0.35	0.66	0.11	15.01	0.61	315.31	0.90	0.05	−1.30	0.17	−0.77	0.27	−0.57	0.48	−0.32	17.70	1.25	<0.001	<0.001
Ni	mg kg^{-1}	0.2–10,000	0.0	11.55	0.79	29.39	0.42	14.89	1.53	12.78	0.72	220.46	1.15	0.70	−0.15	3.20	0.51	5.70	0.76	10.40	1.02	596.00	2.78	<0.001	<0.001
Pb	mg kg^{-1}	0.2–10,000	0.0	10.26	0.91	7.70	0.30	19.47	1.55	2.61	−0.03	13.79	−0.22	1.10	0.04	5.00	0.70	8.20	0.91	13.40	1.13	80.10	1.90	<0.001	0.302
Sn	mg kg^{-1}	0.2–500	2.2	0.69	−0.27	0.57	0.30	1.09	0.36	3.76	0.11	25.5	0.10	<0.2	−1.00	0.30	−0.52	0.50	−0.30	0.90	−0.05	6.10	0.79	<0.001	<0.001
V	mg kg^{-1}	1 - 10,000	0.0	45.25	1.43	56.96	0.44	73.44	2.31	3.64	0.14	20.28	−0.31	2.00	0.30	13.00	1.11	26.00	1.41	53.00	1.72	552.00	2.74	<0.001	0.033
Zn	mg kg^{-1}	2 - 10,000	0.1	25.04	1.26	31.11	0.32	38.76	1.78	5.71	0.35	40.26	1.69	<2	0.00	12.00	1.08	18.00	1.26	27.00	1.43	304.00	2.48	<0.001	<0.001

Note: Concentrations are expressed in mg kg^{-1} and atomic percentage (at.%); RD = Raw data; Log_{10} = Log_{10} transformed data; LLD - ULD = lower and upper limits of detection; SD = standard deviation; MAD = median absolute deviation; SKEW = skewness; Rku = kurtosis; Min = minimum; Q1 = 1st quartile; M = median; Q3 = 3rd quartile; Max = maximum; p.Lt = p value of the Lilliefors test.

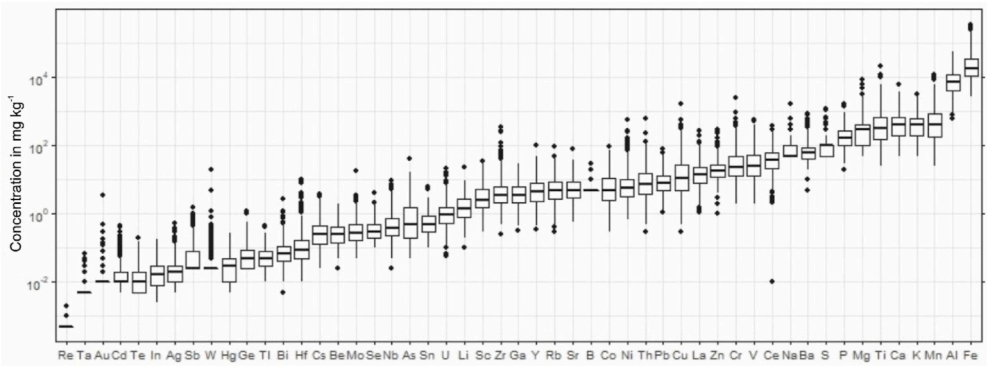

Fig. 5. Comparison of boxplots for 51 elements in active stream sediments of the IRW after aqua regia digestion ordered by increasing median value in mg kg^{-1} converted to log_{10} transformed data.

constructed for six selected elements (Cu, Mo, Fe, Mn, Ni, and Cr) in stream sediments of the IRW, showing also both the UBL and the LBL estimated by a variety of methods (cf. Table 2) for each of the referred elements (Fig. 8). CP plots for all 51 elements are provided in the supplementary material (Fig. 8SM), however only threshold values are indicated.

A comparison of reference levels for PTE (e.g., As, Cd, Cr, Cu, Hg, Ni, Pb, and Zn) contemplated in the Brazilian regulation (CONAMA, 2012) in stream sediments, the threshold concentrations obtained for IRW area and different study cases around the world (Albanese et al., 2007; Cheng et al., 2014; Costa et al., 2015; Larizzati et al., 2014, 2018; Mineropar, 2001; Rodrigues et al., 2013; Salomão et al., 2019b; Teng et al., 2009) is provided in Table 3. Some characteristics of those studies were highlighted as important for the interpretation and comparison, for instance: the area of investigation (km^2), the sample size (n), the particle size (mm) submitted for analysis and the analytical and statistical approach for deriving concentration values. In addition, intervention limits established by the Brazilian (CONAMA, 2012), the Canadian (Canadian Council of Ministers of the Environment - CCME, 2001), the Dutch (Hin et al., 2010), the Australian (Department of Environment and Conservation - DEC, 2010) and the New Zealand (Australian and New Zealand Environment and Conservation Council - ANZECC and Agriculture and Resource Management Council of Australia and New Zealand - ARMCANZ, 2000) environmental legislation are compared, as well as, additional freshwater sediment quality guidelines (SQGs) (Environment Canada - EC and Ministere de l'Envionnement du Quebec - MENVIQ, 1992; Hin et al., 2010; Long and Morgan, 1990; MacDonald et al., 2000; Persaud et al., 1993; Smith et al., 1996) that have been based on various approaches, are also presented in Table 3.

Note: AR = aqua regia; EDTA5% = Ethylenediaminetetraacetic acid; ICP-MS = Inductively coupled plasma-mass spectrometry; ICP-OES = inductively coupled plasma optical emission spectrometry; XRF = X-ray fluorescence; 75th = 75th percentile; MAD = Median +2*Median Absolute Deviation; TIF = Tukey Inner Fence; MAA = Multiple Analytical Approaches; ELA = effects level approach; ERA = effects range approach; SLCA = screening level concentration approach; '*' = Data extracted from; '†' = Compiled by '-' = Not applicable or not mentioned.

5. Discussions

5.1. Regional distribution of selected elements in the IRW

IDW interpolation and microcatchment-based distribution maps of selected elements in stream sediments of the IRW presented (Fig. 6) can assist in defining dominant regional geochemical trends. From that as well as geological data (Fig. 2b), it is also evident that positive and negative anomalies are mostly related to the geotectonic domains of the region and dominant local lithologies.

The Carajás Mineral Province hosts a large variety of polymetallic ore deposits (Gibbs et al., 1986). Reviews addressing the general aspects (Grainger et al., 2008; Xavier et al., 2012) and compilations of geochronological data and metallogenesis (Melo et al., 2016; Moreto et al., 2015, 2014) of copper deposits in Carajás provide a general overview on Cu–Au mineralization origin in the Carajás Domain. The Iron Oxide Copper Gold (IOCG) ore deposits are mostly arranged along two main zones called Northern (Cinzento Fault, 2.57 Ga; e.g., Salobo, Paulo Afonso, GT46/Igarapé Cinzento, Grota Funda, Serra Verde, and Furnas; Melo et al., 2016) and Southern (Canaã Fault, 2.72–2.68 Ga; e.g., Sossego, Cristalino, Bacaba, 118, Castanha, and Estrela; Monteiro et al., 2008; Moreto et al., 2015, 2014) copper belts. These two copper mineralized belts are clearly registered in the stream sediment geochemical data of Cu (Figs. 6 and 7). Anomalous values are also observed for Sn and Mo in similar areas (Figs. 6 and 6SM), which suggests that their enrichments are related to the same hydrothermal alteration processes responsible for Cu-mineralization.

Higher concentrations of Fe (Figs. 6 and 7SM) are mainly observed in the Carajás basin in areas of occurrence of continental meta-tholeiitic basalts and rhyolites (Parauapebas Formation), associated with BIF and volcanogenic sediments (Carajás Formation). The world-class iron deposits of Carajás (e.g., N4, N5, S11D) are related to the ferruginous crusts associated with the Carajás Formation. High anomalous values of Fe were also registered in the Bacajá Domain, and are mainly associated with the Tapirarapé metamafic rocks and Buritirama metavolcanosedimentary sequences. Additionally, minor Cu–Zn disseminated volcanogenic deposits (e.g., Pojuca) are also reported in the area and are coincident with the higher values of Zn in the basin (Fig. 6SM and 7).

Nickel, Cr, and Co exhibit a similar spatial distribution and occur in all four main geologic domains of the IRW (Figs. 6 and 6SM). These metals are commonly associated and it is well-known their relationship with occurrences of mafic-ultramafic layered intrusions (Salminen et al., 1998; Ure and Berrow, 1982). In the IRW, Ni, Cr, and Co are linked to the Cateté Suite, which includes the Onça, the Puma, the Vermelho, and the Luanga complexes (Machado et al., 1991; Mansur and Ferreira Filho, 2017; Rosa, 2014) and, in a minor degree, with the metavolcanic sequences of the Itacaiúnas Supergroup, the Mesoarchean Sapucaia greenstone belt (Sousa et al., 2015; Vasquez et al., 2008), the Neoarchean Serra do Tapa and the Quatipuru mafic-ultramafic complexes of the Araguaia belt and, in the Bacajá domain, with the Tapirapé metamafic rocks and mafic granulites (Figs. 2 and 6). The Onça-Puma Ni mines are situated in the southwestern area of the IRW in the RM-S-CC domains.

Patterns of Mn distribution are similar to those of Ni, Cr, and Co. However, the most prominent Mn concentrations are situated in the BD (Fig. 6), which contains several Mn deposits, as well as the Buritirama Mn mine, mostly related to the Buritirama formation (CPRM, 2018; Salgado et al., 2019; Vasquez et al., 2008). The Azul Mn mine is located

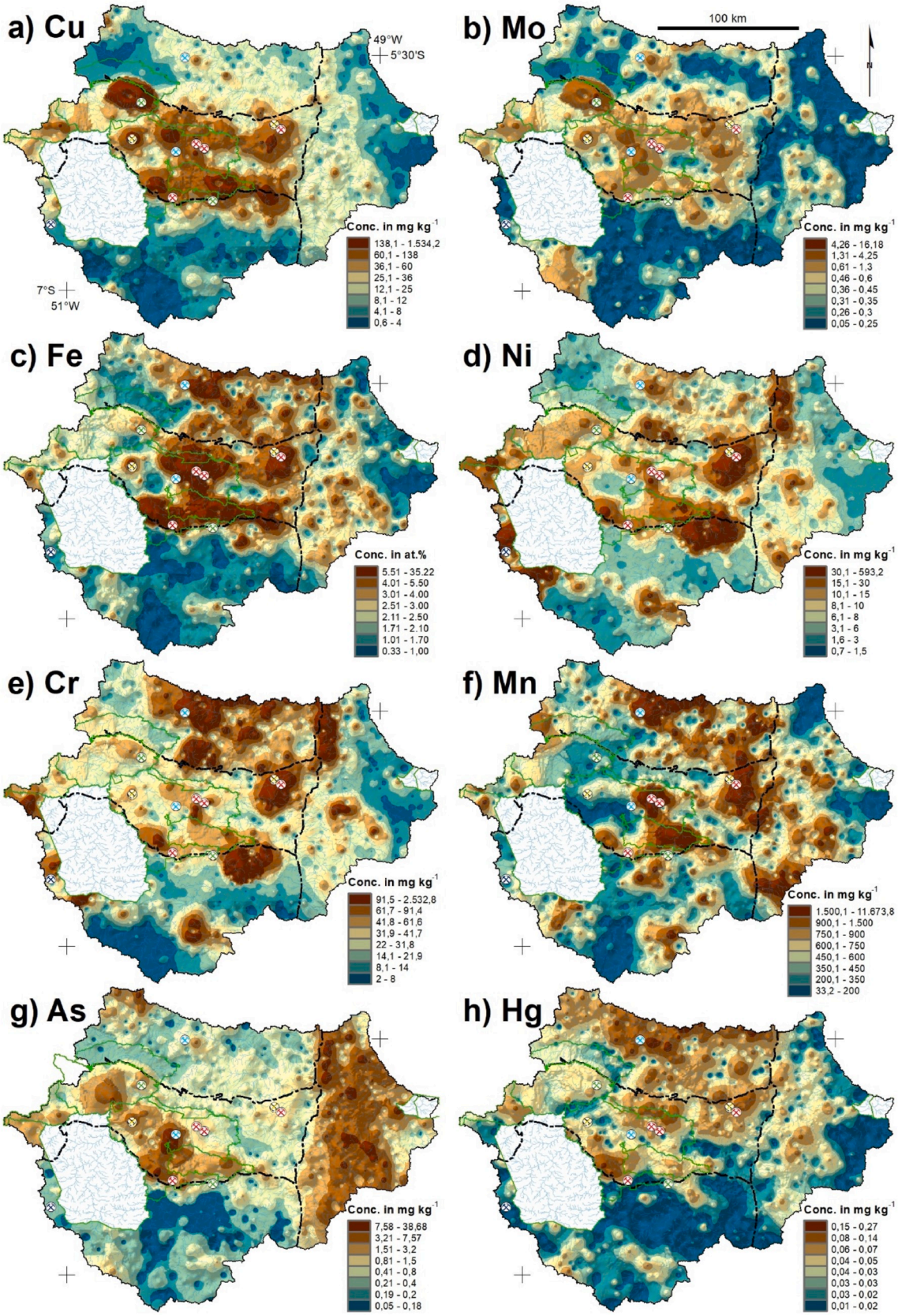

Fig. 6. Inverse distance weighting distribution maps of (a) Cu, (b) Mo, (c) Fe, (d) Ni, (e) Cr, (f) Mn, (g) As and (h) Hg in the Itacaiúnas River Watershed. Dashed black line indicates geotectonic boundaries (refer to Fig. 2).

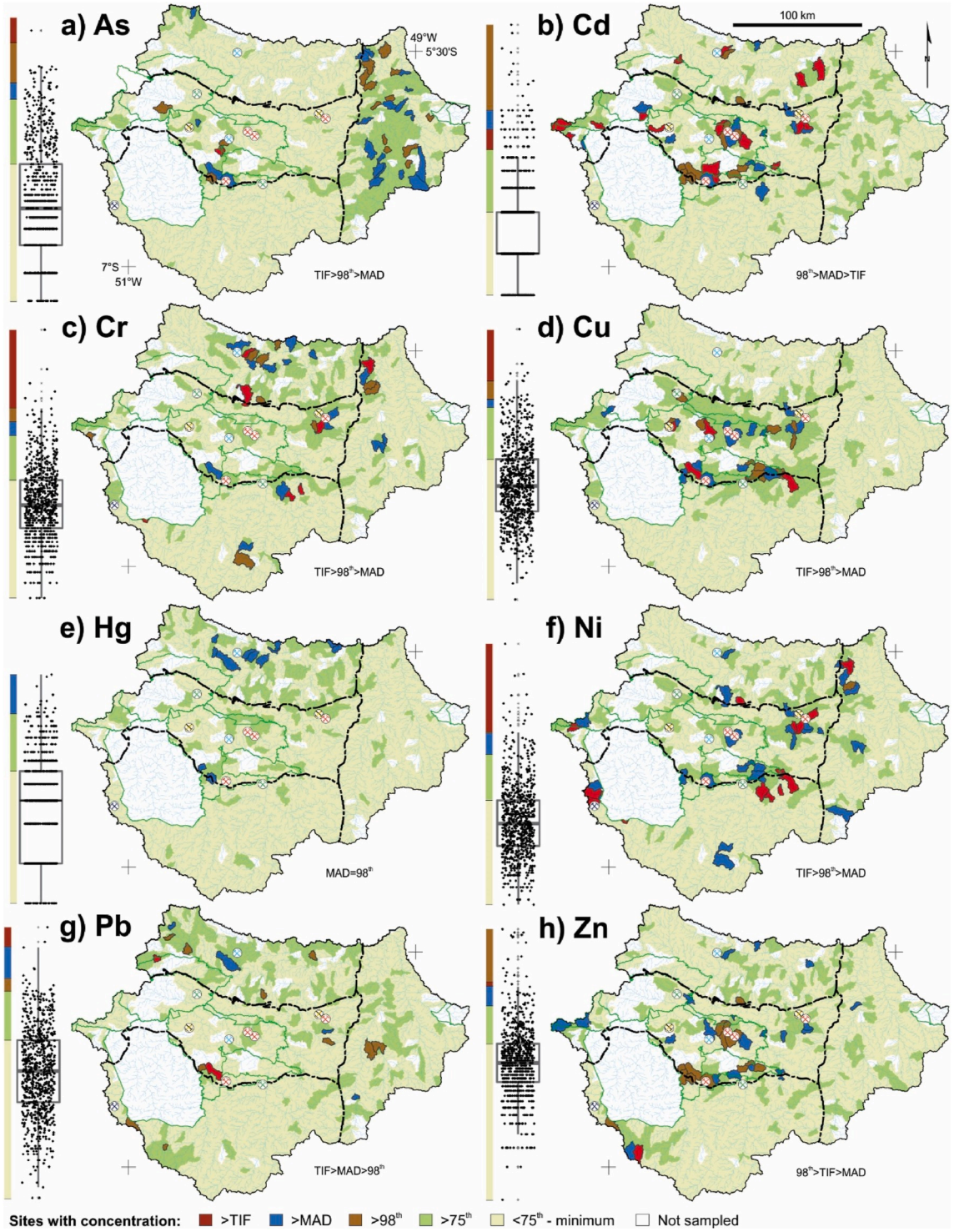

Fig. 7. Geochemical distribution maps for (a) As, (b) Cd, (c) Cr, (d) Cu, (e) Hg, (f) Ni, (g) Pb and (h) Zn showing catchments with concentration > UBL (threshold) in IRW estimated by a variety of methods: Tukey Inner Fence (TIF), Median ± 2*Median Absolute Deviation (MAD), and the 98th percentile. Refer to Table 3 for the calculated UBL values. Dashed black line indicates geotectonic boundaries (refer to Fig. 2). Inverse distance weighting distribution maps for the same elements are presented in Fig. 6 (Cr, Cu and Ni) or in Fig. 7SMa.

in the Carajás basin were high anomalous contents of Mn are also observed. The same is true in the Araguaia belt, particularly in the upper courses of the Vermelho and Sororó rivers. This local enrichment in Mn could be related to geomorphological/pedological characteristics of the AB. A previous study about the spatial distribution of heavy metals in surface water of Vermelho and Sororó rivers (Salomão et al., 2018, Fig. 1) revealed that the concentrations of Fe and Mn in those water bodies are exceptionally high and are controlled by biogeochemical processes and geomorphological features. During weathering processes, Mn and Fe are released into streams in detrital phases and/or as secondary Mn^{4+} oxides that form either discrete concretions or surface coatings on primary minerals and lithic fragments (Salminen et al., 2006).

The arsenic distribution in the IRW is markedly distinct from that of

Table 2
Threshold concentration of 14 selected PTE and Fe in 761 stream sediment sites of the IRW estimated by a variety of methods: Tukey Inner Fence (TIF), Median ± 2*Median Absolute Deviation (MAD), and percentile based background (98th, 95th, 90th and 75th). The number of samples above the upper background limit (UBL) is presented. Table 2SM in Supplementary material has information for all 51 elements.

Elements	Geochemical background values for the Itacaiúnas River Watershed						Number of samples above UBL, n>					
	TIF	MAD	98th	95th	90th	75th	TIF	MAD	98th	95th	90th	75th
As	30.81	7.57	11.38	7.4	4.30	1.5	1	37	16	38	76	187
Ba	303.75	199.66	257.97	180.0	140.0	90.0	9	34	16	37	76	185
Cd	0.06	0.08	0.11	0.08	0.04	0.02	55	39	12	27	72	172
Co	96.97	44.07	46.05	28.90	21.10	10.8	1	17	16	38	75	190
Cr	323.09	154.78	224.40	140.00	90.00	47.0	7	30	16	37	76	188
Cu	320.30	138.15	178.70	118.50	69.40	26.40	6	31	16	38	76	190
Fe	21.16	10.65	13.06	8.48	6.11	3.55	4	25	16	37	76	190
Hg	**0.56**	0.14	0.14	0.11	0.08	0.05	0	17	12	30	73	151
Mn	7862.79	3759.73	3368.0	2100.0	1520.0	837.0	5	11	16	38	76	189
Mo	2.28	1.27	2.01	1.18	0.85	0.48	14	34	16	38	75	189
Ni	60.93	33.90	59.04	36.0	21.40	10.40	15	42	16	38	76	190
Pb	58.79	35.55	29.08	25.4	20.4	13.40	2	6	16	36	76	188
Sn	4.68	2.27	2.18	1.70	1.3	0.9	3	14	16	37	66	147
V	436.29	203.04	213.17	151.0	110.0	53.0	2	17	16	38	76	187
Zn	91.12	59.90	99.77	59.0	43.0	27.0	17	38	16	38	70	180

Note: Iron concentration is expressed in atomic percentage (at.%) and the remaining elements in mg kg^{-1}. '**Bold**' UBL > maximum.

other chemical elements. It shows higher concentrations in the Araguaia belt and in some areas of the Carajás basin, while is extremely depleted in the Mesoarchean domains of the southern IRW (Fig. 6). The enrichment of As in the AB may be related to the occurrences of carbon-rich cherty phyllites and graphite schists located at the western part of the AB (Moura et al., 2008; Paixão and Gorayeb, 2014; Villas et al., 2007). Arsenic will remain mobile in water (As^{3+}) only if pH and Eh are low (Wedepohl, 1978), which is not the case for the AB region, where measured pH values are near neutral to moderately alkaline (between 6 and 8; Salomão et al., 2018). Besides, under the surface-oxidized conditions prevalent in the AB, the small amount of dissolved As (<1 μg/L) is rapidly oxidized onto As^{5+} (insoluble) and becomes adsorbed to hydrous oxides of Fe and Mn, naturally abundant in the region (Salomão et al., 2018) or onto potassic clays (Melo et al., 2007) and organic matter (Ure and Berrow, 1982).

Mercury contents in the stream sediments of IRW are not high (<0.27 mg kg^{-1}; Fig. 6) and the lowest values are registered in the Mesoarchean domains of southern IRW and in the AB to the east. Comparatively higher concentrations of Hg are observed in the CB and in the BD. The anomalous values of Hg in the CB are more probably related to the hydrothermal mineralized zones of the northern and southern copper belts (Fig. 6), as Hg can occur as a trace constituent in some sulphide minerals (Kabata-Pendias and Pendias, 2001; Salminen et al., 2006). Those anomalous values from the BD are not easily understood.

The regional distribution of the selected elements indicates a pronounced control on stream sediment geochemistry by the underlying geologic setting and catchment lithology. The geochemical maps (Figs. 6 and 6SM), give not only valuable information for selecting potential areas for mineral exploration surveys, but also for evaluating geochemical contaminant effects with time-varying treatments.

5.2. Geochemical background of the IRW

GB values determined in this study demonstrate the large variations of elemental concentrations in stream sediments of the IRW. Diversified statistical methods were used to derive GB concentrations and they provided different results, showing commonly a wide range of values (Table 2). By assuming that a single threshold value derived from a specific method will not necessarily represent the study area, not only because of the specificities of each method, but also due to the accentuated variations of background in space reflecting the strong imprint of geologic domains (Figs. 6 and 7). Statistical techniques proposed in the literature (Ander et al., 2013; Cembranel et al., 2017; Reimann et al., 2018, 2005; Reimann and Caritat, 2017, 2005; Salomão et al., 2018) were applied in this study. One reason behind some wide differences between the results given by each statistical method is linked to the different central criterion inherent to these methods and its influence in the obtained GB values. For instance, the TIF relies on the 75th percentile (i.e., the Q3 quartile) and the (IQR of the log_{10}-transformed data, whereas the MAD has its central criterion related to the median and the median deviation of the data distribution. On the other hand, percentile-based approaches deliver a fixed number of sites for each element that needs attention. In the case of the stream sediment of the IRW, for the 98th, 95th, 90th, and 75th methods, respectively, a maximum of 16, 38, 76 and 190 sites presented anomalous values and hypothetically should need attention (Table 2). However, percentile-based approaches do not present a valid scientific explanation on why 2, 5 or 10% of the samples should be considered as 'anomalous' regardless of the statistical data distribution (Reimann et al., 2018). Additionally, as most of the GB values are usually greater than the 90th percentile, presenting the 90th, 95th, and 98th percentiles is important because they are reference concentrations to evaluate background values derived from other methods. Besides, these percentile-based values are employed by some environmental agencies to define threshold (Ander et al., 2013; Reimann and Caritat, 2017). In the case of Brazil, CONAMA (2012, 2009, 2004) suggests the use of the 90th and the 75th percentiles to derive quality reference values.

In general, threshold values obtained for the stream sediment dataset of IRW follow either the ordered sequences TIF > MAD>98th or TIF>98th > MAD (cf. Tables 1 and 2), similarly to what was observed in other studies (Reimann et al., 2018; Reimann and Caritat, 2017; Sahoo et al., 2019a; Salomão et al., 2018, 2019b). An exception is observed for Zn, for which GB values presented the order 98th > TIF > MAD>95th (Table 2). Additionally, MAD values generally are greater than the 95th percentile, however, for Cd, Ni, Zr, and Hf, MAD fluctuates between the 90th and the 95th percentiles (Tables 2 and 2SM).

According to Reimann et al. (2018), the TIF method depends only on the data distribution and allows the definition of background values even if no outliers are present in the data set. In other words, the obtained UBL or threshold can be greater than the maximum value obtained in the dataset (e.g., Al, Be, Ga, Hg, and In; Tables 1SM and 2SM), as it extrapolates the 75th percentiles of the data's structure.

When comparing the different statistical methods to derive GB values, it is evident that the 75th percentile is not suitable for this purpose. The anomalous values obtained by this method are too elevated and do not reflect the stream sediment environmental contamination in the IRW. For instance, in the case of As (Fig. 7a), if we consider the 75th

Table 3
A comparison of reference levels for toxic elements in stream sediments of the IRW (in bold), different study cases around the world, intervention limits established by Brazilian, Canadian, Dutch, Australian and New Zealand law, and additional published freshwater sediment quality guidelines (SQGs).

Source	Region (Country) - Project	Area of Investigation (km^2)	Sample size (n)	Particle size (mm)	Approach	Concentration levels expressed in mg kg^{-1}							
						As	Cd	Cr	Cu	Hg	Ni	Pb	Zn
Present study	**IRW (PA-Brazil) – ItacGMBP**	**42,000.0**	**761**	0.177	**AR/ICP-MS/75th**	**1.50**	**0.02**	**47.00**	**26.40**	**0.05**	**10.40**	**13.40**	**27.00**
Present study	**IRW (PA-Brazil) – ItacGMBP**	**42,000.0**	**761**	0.177	**AR/ICP-MS/MAD**	**7.57**	**0.08**	**154.78**	**138.15**	**0.14**	**33.90**	**35.55**	**59.90**
Present study	**IRW (PA-Brazil) – ItacGMBP**	**42,000.0**	**761**	0.177	**AR/ICP-MS/TIF**	**30.81**	**0.06**	**323.09**	**320.30**	**0.56**	**60.93**	**58.79**	**91.12**
(Salomão et al., 2019b)	Southern IRW (PA-Brazil) – CPRM's projects (Total area)	9650.0	689	0.177	AR/ICP-MS/75th	<1.0	0.01	25.0	11.8	0.01	5.6	4.9	10.0
(Salomão et al., 2019b)	Southern IRW (PA-Brazil) – CPRM's projects (Total area)	9650.0	689	0.177	AR/ICP-MS/MAD	<1.0	<0.01	61.01	34.48	<0.01	12.75	10.02	19.97
(Salomão et al., 2019b)	Southern IRW (PA-Brazil) – CPRM's projects (Eastern Carajás region)	2720.0	185	0.177	AR/ICP-MS/MAD	<1.0	<0.01	165.01	244.36	<0.01	34.45	9.4	19.97
(Salomão et al., 2019b)	Southern IRW (PA-Brazil) – CPRM's projects (Sapucaia region)	6930.0	504	0.177	AR/ICP-MS/MAD	<1.0	<0.01	53.89	20.64	<0.01	10.32	8.68	19.97
(Larizzati et al., 2014, 2018)	Quadrilátero Ferrífero (MG-Brazil) - CPRM's projects	45,000.0	3662	0.175	AR/ICP-MS/75th	3.9	0.05	96.30	28.38	63.0	25.20	23.42	43.0
(Costa et al., 2015)	Quadrilátero Ferrífero (MG-Brazil)	7000.0	512	0.063	AR/ICP-OES/75th	5.09	–	–	–	–	–	–	–
(Mineropar, 2001)	Curitiba (PR-Brazil)	2750.0	392	0.162	EDTA5%/ICP-MS/75th	2.5	–	0.5	6.4	25.0	2.7	7.40	9.9
(Albanese et al., 2007)	Siliciclastic deposits of the Campania region (Italy)	13,600.0	2389	0.150	AR/ICP-MS/75th	10.2	0.43	28.0	40.0	67.0	–	29.0	82.0
(Albanese et al., 2007)	Volcanoclastic deposits of the Campania region (Italy)	13,600.0	2389	0.150	AR/ICP-MS/75th	13.9	0.69	28.0	40.0	205.0	–	51.0	156.0
(Teng et al., 2009)	Dexing area (China)	4800.0	326	2.0	MAA/75th	14.0	0.2	36.0	23.0	0.07	–	27.0	72.0
(Cheng et al., 2014)	Southern China - Regional Geochemistry-National Reconnaissance (RGNR)	2,300,000.0	5244	0.074	MAA/75th	19.0	398.0	87.0	34.0	116.0	38.0	41.0	99.0
(Zheng et al., 2014)	Xigaze district (southern Tibet) – RGNR	76,170.0	517	–	MAA/75th	20.64	–	–	37.96	–	–	31.29	87.07
(Zheng et al., 2014)	Xigaze district (southern Tibet) – RGNR	76,170.0	517	–	MAA/MAD	32.68	–	–	56.52	–	–	43.71	114.31
(Zheng et al., 2014)	Xigaze district (southern Tibet) – RGNR	76,170.0	517	–	MAA/TIF	54.21	–	–	–	–	–	57.82	142.52
(Gallagher et al., 2016)	Northern Counties of Ireland - Tellus and Tellus Border Projects	26,200.0	9471	2.0	Pressed pellet/XRF/75th	15.5	0.8	186.0	45.0	–	76.4	36.2	167.0
(Reimann and Caritat, 2017)	Australia - National Geochemical Survey of Australia (NGSA) Top Outlet Sediment (Tc; 0–10 cm)	6,174,000.0	1313	2.0	AR/ICP-MS/75th	2.9	0.07	37.4	18.0	0.03	17.0	11.2	43.5
(Reimann and Caritat, 2017)	Australia - NGSA's Bottom Outlet Sediment (Bc; ~60–80 cm)	6,174,000.0	1314	2.0	AR/ICP-MS/75th	3.4	0.05	39.7	18.38	0.02	18.5	10.9	41.8
(Reimann and Caritat, 2017)	Australia - NGSA's Top Outlet Sediment (Tc; 0–10 cm)	6,174,000.0	1313	2.0	AR/ICP-MS/MAD	3.4	0.1	44.0	24.0	0.01	21.0	14.0	55.0
(Reimann and Caritat, 2017)	Australia - NGSA's Top Outlet Sediment (Tc; 0–10 cm)	6,174,000.0	1313	2.0	AR/ICP-MS/TIF	16.8	0.5	149.0	109.0	0.29	121.0	53.0	254.0
(CONAMA, 2012)	Brazil - L1	–	–	–	*(CCME, 2001)	5.9	0.6	37.3	35.7	0.17	18.0	35.0	123.0
(CONAMA, 2012)	Brazil - L2	–	–	–	*(CCME, 2001)	17.0	3.5	90.0	197.0	0.486	35.9	91.3	315.0
(CCME, 2001)	Canada - ISQG	–	–	–	*(MacDonald et al., 2000)	5.9	0.6	37.3	35.7	0.17	18.0	35.0	123.0
(CCME, 2001)	Canada - PEL	–	–	–	*(MacDonald et al., 2000)	17.0	3.5	90.0	197.0	0.486	35.9	91.3	315.0
(DEC, 2010)	Australia - ISQG-Low	–	–	–	*(ANZECC and ARMCANZ, 2000)	20.0	1.5	80.0	65.0	0.15	21.0	50.0	200.0
(DEC, 2010)	Australia - ISQG-High	–	–	–	*(ANZECC and ARMCANZ, 2000)	70.0	10.0	370.0	270.0	1.0	52.0	220.0	410.0

(*continued on next page*)

Table 3 (*continued*)

Source	Region (Country) - Project	Area of Investigation (km^2)	Sample size (n)	Particle size (mm)	Approach	Concentration levels expressed in mg kg^{-1}							
						As	Cd	Cr	Cu	Hg	Ni	Pb	Zn
(ANZECC and ARMCANZ, 2000)	Australia and New Zealand - ISQG-Low	–	–	–	*(Long et al., 1995)	20.0	1.5	80.0	65.0	0.15	21.0	50.0	200.0
(ANZECC and ARMCANZ, 2000)	Australia and New Zealand - ISQG-high	–	–	–	*(Long et al., 1995)	70.0	10.0	370.0	270.0	1.0	52.0	220.0	410.0
(Hin et al., 2010)	Netherlands – Intervention values	–	–	–	MAA	85.0	14.0	380.0	190.0	10.00	210.0	580.0	2000.0
(Smith et al., 1996)	Threshold effect level (TEL) - Threshold Effect Concentrations (TEC)	–	–	–	ELA/†(MacDonald et al., 2000)	5.9	0.6	37.3	35.7	0.17	18.0	35.0	123.0
(Persaud et al., 1993)	Lowest effect level (LEL) – (TEC)	–	–	–	SLCA/†(MacDonald et al., 2000)	6.0	0.6	26.0	16.0	0.20	16.0	31.0	120.0
(EC and MENVIQ, 1992)	Minimal effect threshold (MET) – (TEC)	–	–	–	SLCA/†(MacDonald et al., 2000)	7.0	0.9	55.0	28.0	0.20	35.0	42.0	150.0
(Long and Morgan, 1990)	Effect range low (ERL) – (TEC)	–	–	–	ERA/†(MacDonald et al., 2000)	33.0	5.0	80.0	70.0	0.15	30.0	35.0	120.0
(MacDonald et al., 2000)	Consensus-Based TEC	–	–	–	MAA	9.79	0.99	43.4	31.6	0.18	22.7	35.8	121.0
(Smith et al., 1996)	Probable effect level (PEL) - Probable Effect Concentrations (PEC)	–	–	–	ELA/†(MacDonald et al., 2000)	17.0	3.53	90.0	197.0	0.486	36.0	91.3	315.0
(Persaud et al., 1993)	Severe effect level (SEL) – (PEC)	–	–	–	SLCA/†(MacDonald et al., 2000)	33.0	10.0	110.0	110.0	2.00	75.0	250.0	820.0
(EC and MENVIQ, 1992)	Toxic effect threshold (TET) – (PEC)	–	–	–	SLCA/†(MacDonald et al., 2000)	17.0	3.0	100.0	86.0	1.00	61.0	170.0	540.0
(Long and Morgan, 1990)	Effect range median (ERM) – (PEC)	–	–	–	ERA/†(MacDonald et al., 2000)	85.0	9.0	145.0	390.0	1.30	50.0	110.0	270.0
(MacDonald et al., 2000)	Consensus-Based PEC	–	–	–	MAA	33.0	4.98	111.0	149.0	1.06	48.60	128.0	459.0

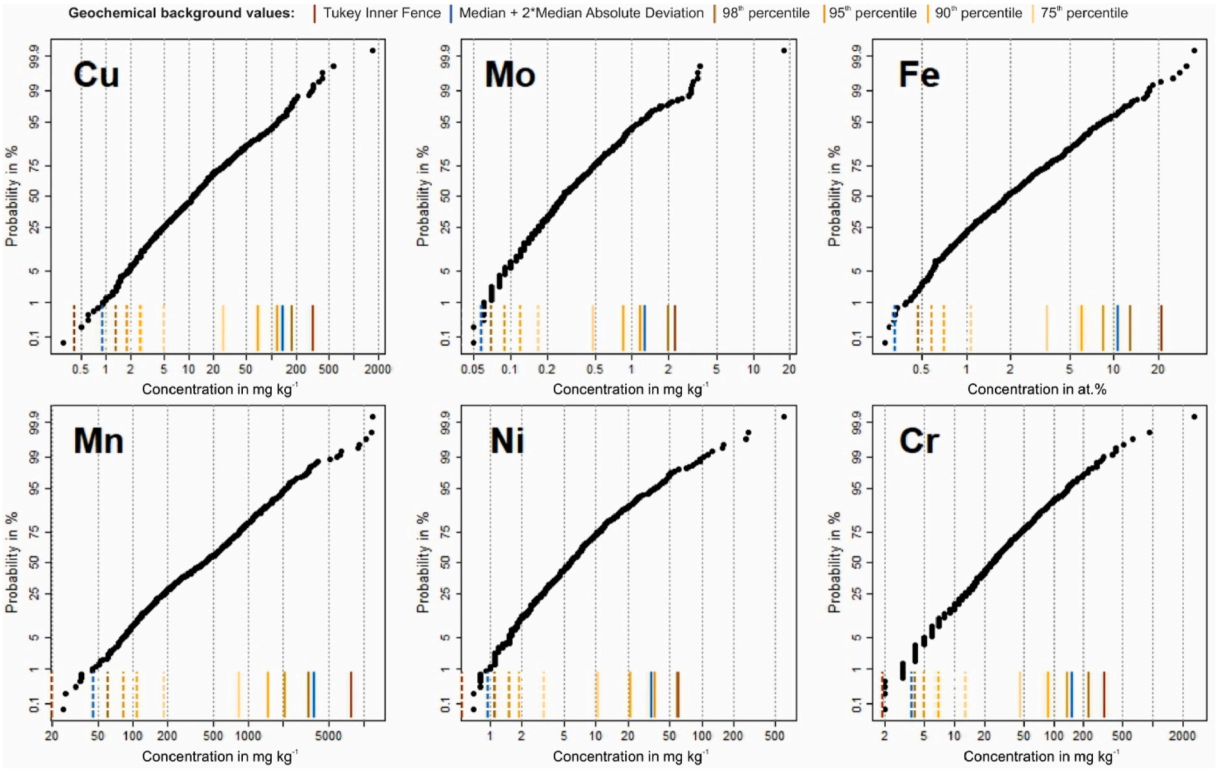

Fig. 8. Cumulative probability (CP) distribution diagrams for six selected elements (Cu, Mo, Fe, Mn, Ni, and Cr), in stream sediments of the IRW. The solid vertical lines are upper background limits and the dashed vertical lines are the lower background limits estimated by a variety of methods (cf. Table 3). CP plots for all 51 elements are provided in the supplementary material, Fig. 8SM.

percentile as a threshold, a large number of sampling sites need attention, particularly in the eastern part of the IRW. However, as discussed previously, the large number of anomalous values observed for As in the Araguaia belt is strongly controlled by the catchment lithology dominant in that geologic domain (Figs. 2 and 6). In fact, the high As values observed are strictly related to natural or geogenic local characteristics and do not necessarily correspond to an environmental problem that needs attention. On the other hand, the strong contrast in As spatial distribution in the IRW indicates the need for calculation of specific values of As background in the different geologic domains of the IRW.

Furthermore, both UBL and LBL derived from the MAD approach correlate well with the major breaks in the CP diagrams (Fig. 8). This suggests that the MAD method can be a valid option in defining threshold instead of applying the subjectivity of the cumulative probability method. Conclusively, for the stream sediment dataset of the ItacGMBP project, we consider that the MAD method gives the most appropriate results for deriving GB values. Sahoo et al. (2019a) reported similar conclusions in the study of GB in soils of the Parauapebas sub-basin of the IRW. The GB values indicated by MAD (Table 2) can be used as references to stablish comparisons between element concentrations in stream sediments of the IRW at the regional scale. However, the MAD method usually gives conservative values when compared with the TIF (Reimann et al., 2018; Reimann and Caritat, 2017) and this aspect should be considered because the number of sites needing attention is comparatively higher. At this point, it should be remembered that the number of sites above the threshold values presented in Table 2 results merely of statistical calculation. Further studies should be undertaken in order to select the real number of sites that truly need attention to ensure the best cost-benefit results.

Finally, as systematically discussed in this study as well as in others (Reimann et al., 2018; Reimann and Caritat, 2017; Sahoo et al., 2019a; Salomão et al., 2018, 2019b), the influence of the local geology on the GB values is remarkable. As a consequence, calculating background concentrations of chemical elements in a given area without considering the geologic setting and lithologies is a simplistic approach. In conclusion, for geological domains showing strong geochemical contrasts, as exemplified by Cu and As spatial distribution in the IRW (Fig. 6), it is more suitable to define different background values than to work with misleading integrated values. A similar approach is highly recommended by the guideline procedures of the Ministry of the Environment of Finland (MEF, 2007).

5.3. *Integrating geochemical maps with background values for the assessment of SQGs*

Microcatchment-based representation of uni-element concentrations in stream sediment based on threshold values for the identification of concentrations above the regional background are provided in Figs. 7 and 7SM. The microcatchments showing anomalous values for environmental concern (higher than TIF, MAD, and 98th) are highlighted and the microcatchments with values > 75th and <75th are also indicated as reference to the understanding of each element behavior in the IRW. This option was done based on the previous discussion on geochemical background of the IRW, which demonstrated that MAD, followed by TIF and 98th, are the preferential methods to define background values and that the 75th percentile should be seen only as conservative reference values.

Among the PTE, for As (Fig. 7a), UBL above 98th and MAD are notably concentrated in the Araguaia belt in the eastern part of the IRW. Other values, higher than TIF, 98th, and MAD, occur sparsely in the Carajás basin. The RM-S-CC domains and Bacajá domain are practically devoid of high anomalous values. Copper (Fig. 7d), Cd (Fig. 7b), Zn (Fig. 7h), and Mo (Fig. 7eSM) values above TIF, 98th, and MAD are concentrated in the Carajás basin and appear to be essentially controlled by the hydrothermal mineralized zones related to the northern and southern copper belts. Chromium (Fig. 7c), Ni (Fig. 7f), and Co

(Fig. 7dSM) values higher than TIF, 98th, and MAD, are dispersed in the IRW and reflect mostly lithological control. Iron (Fig. 7aSM) anomalous values are concentrated in the Carajás basin and controlled by the ferruginous crusts derived from banded iron formations. Manganese anomalies (Fig. 7bSM) are also observed in the Carajás basin but are remarkable in the Bacajá domain. Vanadium (Fig. 7gSM) apparently behaves similarly to Mn. Barium anomalies mainly occur in the BD, CB and RM-S-CC domains (Fig. 7cSM). Tin anomalies are scarce (Fig. 7fSM) and possibly related to the occurrence of Paleoproterozoic anorogenic granites in the IRW. Mercury (Fig. 7e) and Pb (Fig. 7g) anomalous values are rare in the IRW and those of Hg are concentrated in the Bacajá Domain.

The central question about all the identified anomalous values of PTE in the IRW is to define: what is the origin and real significance of these anomalies in environmental grounds? All presented evidence about the elemental geochemistry in the IRW point to a dominant influence of geotectonic domains and local lithologies better than to anthropogenic effects. SQGs have been proposed in a wide range of studies in different continents (Table 3). The SQGs are proposed to define pollutant concentrations in stream sediments and to evaluate their relationship to any adverse effect resulting from the exposure to contaminants (CCME, 2001). The determination of SQGs can be acquired by several methods (cf., MacDonald et al., 2000; and references therein; Table 3). The approaches that have been selected by individual jurisdictions basically depend on four aspects (CCME, 1995; Doğan-Sağ;lamtimur and Kumbur, 2010): i) the receptors to be considered; ii) the degree of protection to be afforded; iii) the geographic area to which the values are intended to apply; and, iv) and their intended uses.

Studies conducted to determine background values are needed for decision making in environmental management. Geochemical background values are important to attest actions in cases of potential contamination. In the absence of these studies, misleading interpretations of the magnitude of contamination levels in a certain area may cause under- or overestimation of GB (Fernandes et al., 2018; Rodrigues et al., 2013). For instance, a high concentration value of a given chemical element for a certain area can correspond to an average or even low concentration value in comparison to another area, and this can be due essentially to contrasts in geological setting and dominant lithologies of the considered areas. For this reason, the use of reference concentrations for a whole continent or large areas in general and/or extrapolating GB values from an area to another one without consideration of their specific geologic settings are not suitable for detailed environmental evaluation. The definition of GB values for PTE in the IRW makes possible a clearer distinction of the real anomalous values for those elements and associate with their spatial distribution in the study area, it can be used as a guide for effective environmental protection.

The majority of GB studies are conducted for soils and surface water media, however, in the case of stream sediments, there is a drastic lack of GB definition in multiple working scales (e.g., continental, regional and local). A Brazilian regulation concerning sediment quality for the protection of the aquatic life is still nonexistent, especially when dealing with PTE (as described here) or organic contaminant. Hence, so far there are no SQGs officially approved by Brazilian environmental agencies, despite the asks for definition of SQGs in the national territory (Almeida and Rocha, 2006; Rodrigues et al., 2013; Soares and Mozeto, 2006).

The only legal resolution in the Brazilian territory that is applied to this topic is that of resolution number 454 (CONAMA, 2012), which establishes general recommendations and reference procedures for the management and disposal of material to be dredged in waters nationwide. That resolution is entirely based in the Canadian legislation (CCME, 2001) and defines two levels (L1 and L2) for the material to be dredged. The L1 in CONAMA, 2012 corresponds to the threshold effect level (TEL in CCME, 2001), which means a threshold value below which low probability of adverse effects to the biota are expected; and L2 (CONAMA, 2012) correlates to probable effect level (PEL in CCME, 2001), which refers to a threshold value above which a probable adverse effect to the biota is expected.

According to CCME (2001), SQGs should be developed from detailed dose-response data from sensitive species of aquatic organisms at a given specific area. Furthermore, the results of these studies should then be validated in field trials to ensure that any SQGs derived from these data are applicable in a broad range of locations and not only in the area where the study was carried out (CCME, 2001; Deckere et al., 2011; Persaud et al., 1993). As the only available Brazilian regulation for SQGs is exclusively based on values determined in Canada (CCME, 2001), it does not consider the accentuated contrasts between different regions and it is not able to define consistent threshold values for the entire Brazilian territory.

The elements presented in Table 3 are commonly considered as potentially toxic elements in different environmental legislations around the world. However, in some cases, other elements are also included. In Australia, DEC (2010) contemplates all eight elements presented in Table 3, as well as Sb (2.0 and 25.0 mg kg^{-1} dry weight for ISQG-low and ISQG-high, respectively) and Ag (1.0 and 3.7 mg kg^{-1} dry weight for ISQG-low and ISQG-high, respectively). In Ontario, guidelines for the protection and management of aquatic sediment quality (Persaud et al., 1993) contemplate additionally Fe (2.0 and 4.0 wt% dry weight for Lowest Effect Level and Severe Effect Level, respectively) and Mn (460 and 1100 mg kg^{-1} dry weight for Lowest Effect Level and Severe Effect, respectively).

In the case of Brazil, for the inclusion of chemical substances not listed in CONAMA, 2012, the environmental licensing body must first establish the guiding values to be adopted in the Brazilian territory according to its specificities. In spite of the proposition of CONAMA, (2012) that background values of a given region will prevail over the national values, whenever they are higher, it is clear that the chosen investigation levels do not reflect the real scenario of the IRW region, neither that of the Brazilian territory.

Assuming MAD calculated values as representative of GB in the IRW, the threshold values for Cr, Cu, and Ni are much higher than those of L1, whereas those of As and Pb are similar to L1, and Cd, Hg, and Zn are significantly lower than the proposed levels (CONAMA, 2012, Table 3). However, as discussed before, there is clear evidence that Cr and Ni enrichment in the IRW is controlled by dominant lithologies (Fig. 6c and d) and that of Cu by the mineralized copper belts strongly enriched in that element. The southern copper belt is situated in the border between the Carajás basin and the RM-S-CC domains (Fig. 6e) and in that area were registered very high concentrations of Cu (244.36 mg kg^{-1}; Salomão et al., 2019b) in comparison to other areas of the IRW. On the other hand, the UBL value obtained for As in the whole watershed (7.57 mg kg^{-1}; Table 3) differs significantly from the extremely low concentrations of As (<1.0 mg kg^{-1}) observed in the RM-S-CC domains in the southern IRW (Salomão et al., 2019b), as well as in the Araguaia belt, located in the eastern area of the IRW, which is marked by comparatively higher As contents (Fig. 6g). This is a strong evidence that the geochemistry of stream sediments and the spatial distribution of chemical elements in the IRW cannot be understood without using the geologic setting and lithological influence as a reference. The behavior of Cu and As illustrates extremely well the strong dependence of variations in concentration and geological domains. Even in the sole context of the IRW, it is clear that it is not consistent to work with uniform values of SQGs. This is even more accurate if we consider all Brazilian territory and the fact that the adopted SQGs derived from the Canada legislation, a country with an entirely distinct environmental and climatic condition, when compared with Brazil.

The IRW (Carajás province) and the Quadrilátero Ferrífero region (QFe; State of Minas Gerais, Brazil) are two examples of strongly mineralized areas, with similar geological setting. The QFe is well known for its high As concentrations (Borba et al., 2004; Costa et al., 2018, 2015; Larizzatti et al., 2018), which can be seen by comparing the values obtained by the 75th percentile-based approach (Table 3) in the IRW (1.50 mg kg^{-1}) and in the QFe (5.09 mg kg^{-1}; Costa et al., 2015).

Moreover, in the QFe, Ni (38.6 mg kg^{-1}) and Zn (68.20 mg kg^{-1}) (Rodrigues et al., 2013) also show greater values in comparison to those of the IRW (Ni = 10.40 mg kg^{-1}; Zn = 27.00 mg kg^{-1}). This illustrates the strong variations of reference values observed in relatively similar provinces.

Lastly, highly industrialized areas from southern China (Cheng et al., 2014), the Dexing area - also in China (Teng et al., 2009), as well as the Xigaze district - in southern Tibet (Zheng et al., 2014) presented extremely higher values for almost all potentially toxic elements in comparison to the IRW (Table 3). This is an additional evidence that the anomalous values observed for some elements in the IRW are not due to anthropogenic effects.

6. Concluding remarks

- The stream sediment geochemical data indicate that there are no evident contamination issues by PTE directly linked to anthropogenic activities at the broad scale of the IRW. High concentration values of Fe and some PTE are essentially linked to local natural sources.
- The geochemical signature in stream sediments is strongly influenced by the geological setting and local lithologies. The geochemical maps of the IRW can provide insights for mineral exploration studies. Higher concentrations of Fe are mainly observed in the Carajás Basin, associated to BIFs and metavolcanic rocks. Copper anomalous values are clearly related to two large Cu hydrothermal mineralized belts located in the Carajás Basin. Nickel, Cr, and Co occur in all four main geologic domains of the IRW, and they are mostly associated with mafic-ultramafic layered intrusions. The most prominent Mn anomalies are situated in the Bacajá Domain, related to the Buritirama Formation. Higher concentrations of As are observed in the Araguaia Belt, related to low-grade metasedimentary rocks.
- The diversified statistical methods used to derive GB concentrations provided a wide range of values. In general, threshold values obtained for the stream sediment dataset of IRW follow either the ordered sequences TIF > MAD>98th or TIF>98th > MAD. It is concluded that the MAD method gives the most appropriate results for deriving GB values.
- The difference in concentration for several elements amongst the four geological domains is remarkable and points to the need of determining different GB values in specific domains, as exemplified by Cu and As.
- Microcatchment-based representation of uni-element concentrations in stream sediment based on threshold values is extremely useful to identify anomalous values (higher than TIF, MAD, and 98th) for environmental concern. This approach reinforced the dominant influence of geotectonic domains and local lithologies better than anthropogenic effects in the IRW. The threshold values for Cr, Cu, and Ni are much higher than those of reference level 1 (L1 – Threshold effect level), as defined by CONAMA in Brazil, those of As and Pb are similar to L1, whereas Cd, Hg, and Zn are significantly lower than L1. It is concluded that it is not suitable to work with uniform values of sediment quality guidelines.
- The knowledge of the natural or geogenic distribution of the elements will definitely assist in defining environmental background values and clean-up levels for ecotoxicological studies.
- Results presented here reflect the actual stream sediment geochemical signature of the IRW, situated in one of the most important mining provinces of South America. Besides its scientific interest, our findings can be useful for Brazil's environmental policy making, e.g., the definition of geochemical guidelines.

Declaration of competing interest

The authors declare that they have no known competing financial interests or personal relationships that could have appeared to influence the work reported in this paper.

Acknowledgements

The ItacGMBP project is currently under execution at Instituto Tecnológico Vale Desenvolvimento Sustentável (ITVDS) with Vale funding (Gerência de Meio Ambiente Corredor Norte). This study was financed in part by the Coordenação de Aperfeiçoamento de Pessoal de Nível Superior – Brasil (CAPES) – Finance Code 001. This work was supported by the Conselho Nacional de Desenvolvimento Científico e Tecnológico (CNPq) [grants 380998/2019–0 to GNS; 306108/2014–3 to RD; 305392/2014–0 to RSA; 443247/2015–3 and 402727/2018–5 projects coordinated by RD]. The authors acknowledge Marcondes Lima da Costa, José Francisco da Fonseca Ramos e José Francisco Bêrredo Reis da Silva for their scientific collaboration with the Background project.

Appendix A. Supplementary data

Supplementary data related to this article can be found at https://doi.org/10.1016/j.apgeochem.2020.104608.

Authors' contributions

GNS processed results, made interpretations and wrote the manuscript assisted by RD, PKS and other co-authors. RSA, CAMF, LRGG and JOS provided extensive advice and performed critical subsequent revisions. JSFJ, PWSF and WRNJ lead project conceptualization and sampling design. MSS and CAMF managed the field work and sampling. MFC and RD guided the project and provided research input and ideas. MFC provided financial support to the project development. All authors contributed to the discussion of the results and to the writing of the manuscript. All authors read and approved the final manuscript.

Data availability

The dataset used for this manuscript is property of Instituto Tecnológico Vale, and will only be available upon request.

References

Albanese, S., De Vivo, B., Lima, A., Cicchella, D., 2007. Geochemical background and baseline values of toxic elements in stream sediments of Campania region (Italy). J. Geochem. Explor. 93, 21–34. https://doi.org/10.1016/j.gexplo.2006.07.006.

Alkmim, F.F. de, 2015. Geological background: a tectonic panorama of Brazil. In: Hermelin, M. (Ed.), Landscapes and Landforms of Colombia. Springer, Dordrecht, pp. 1–210. https://doi.org/10.1007/978-3-319-11800-0.

Almeida, C.A., Rocha, O., 2006. Estudo Comparativo da Qualidade dos Sedimentos dos Reservatórios do Rio Tietê (SP). J. Brazilian Soc. Ecotoxicol. 1, 141–145. https://doi.org/10.5132/jbse.2006.02.010.

Alvarenga, C.J.S., Moura, C.A.V., Gorayeb, P.S.S., Abreu, F.A.M., 2000. Paraguay and Araguaia belts. In: Cordani, U.G., Milani, E.J., Thomas Filho, A., Campos, D.A. (Eds.), Tectonic Evolution of South America. 31st International Geological Congress. Rio de Janeiro, pp. 183–193.

Alvares, C.A., Stape, J.L., Sentelhas, P.C., Moraes Gonsalves, J.L., Sparovek, G., 2013. Koppen's climate classification map for Brazil. Meteorol. Z. 22, 711–728. https://doi.org/10.1127/0941-2948/2013/0507.

Ander, E.L., Johnson, C.C., Cave, M.R., Palumbo-Roe, B., Nathanail, C.P., Lark, R.M., 2013. Methodology for the determination of normal background concentrations of contaminants in English soil. Sci. Total Environ. 454 (455), 604–618. https://doi.org/10.1016/j.scitotenv.2013.03.005.

Australian and New Zealand Environment and Conservation Council - ANZECC, Agriculture and Resource Management Council of Australia and New Zealand - ARMCANZ, 2000. Aust. Gov. Initiat.. Water quality guidelines [WWW Document]. Aust. Gov. Initiat. URL. http://www.waterquality.gov.au/anz-guidelines/resources/previous-guidelines/anzecc-armcanz-2000

Barros, C.E.M., Sardinha, A.S., Barbosa, J.P.O., Macambira, M.J.B., Barley, P., Boullier, A., 2009. Structure, petrology, geochemistry and zircon U/Pb and Pb/Pb geochronology of the synkinematic Archean (2.7 Ga) A-type Granities from the Carajás Metallogenic Province, Northern Brazil. Can. Mineral. 47, 1423–1440.

Bonham-Carter, G.F., Rogers, P.J., Ellwood, D.J., 1987. Catchment basin analysis applied to surficial geochemical data, Cobequid Highlands, Nova Scotia. J. Geochem. Explor. 29, 259–278. https://doi.org/10.1016/0375-6742(87)90081-1.

Borba, R.P., Figueiredo, B.R., Cavalcanti, J.A., 2004. Arsênio na água subterrânea em Ouro Preto e Mariana, Quadrilátero Ferrífero (MG). Rem 57, 45–51. https://doi.org/10.1590/S0370-44672004000100009.
Canadian Council of Ministers of the Environment - CCME, 2001. Canadian sediment quality guidelines for the protection of aquatic life [WWW Document]. Can. Environ. Qual. Guidel. http://ceqg-rcqe.ccme.ca/en/index.html#void (accessed 3.1.19).
Canadian Council of Ministers of the Environment - CCME, 1995. Protocol for the Derivation of Canadian Sediment Quality Guidelines for the Protection of Aquatic Life - Report CCME EPC-98E. Ottawa.
Caritat, P., Cooper, M., 2016. A continental-scale geochemical atlas for resource exploration and environmental management: the National Geochemical Survey of Australia. Geochem. Explor. Environ. Anal. 16, 3–13. https://doi.org/10.1144/geochem2014-322.
Caritat, P., Cooper, M., Lech, M., McPherson, A., Thun, C., 2009. National Geochemical Survay of Australia: Sample Preparation Manual. Geoscience Australia.
Carranza, E.J.M., 2011. Analysis and mapping of geochemical anomalies using logratio-transformed stream sediment data with censored values. J. Geochem. Explor. 110, 167–185. https://doi.org/10.1016/j.gexplo.2011.05.007.
Carranza, E.J.M., Hale, M., 1997. A catchment basin approach to the analysis of reconnaissance geochemical-geological data from Albay Province, Philippines. J. Geochem. Explor. 60, 157–171. https://doi.org/10.1016/S0375-6742(97)00032-0.
Cave, M.R., Johnson, C.C., Ander, E.L., Palumbo-Roe, B., 2012. Methodology for the determination of normal background contaminant concentrations in English soils. Br. Geol. Surv. Comm. Rep. CR/ 12/003, 42.
Cembranel, A.S., Sampaio, S.C., Remor, M.B., Gotardo, J.T., Dalla Rosa, P.M., 2017. Geochemical background in an oxisol. Eng. Agric. 37, 565–573. https://doi.org/10.1590/1809-4430-Eng. Agric.v37n3p565-573/2017.
Cheng, Z., Xie, X., Yao, W., Feng, J., Zhang, Q., Fang, J., 2014. Multi-element geochemical mapping in Southern China. J. Geochem. Explor. 139, 183–192. https://doi.org/10.1016/j.gexplo.2013.06.003.
Companhia de Pesquisa de Recursos Minerais - CPRM, 2018. Atlas of Mineral Deposits and Selected Mineral Occurences of Continental Brazil. CPRM, Brasília.
Companhia de Pesquisa de Recursos Minerais - CPRM, 2013. Projeto metalogenia das províncias minerais do Brasil: área Sapucaia [WWW Document]. URL. http://geosgb.cprm.gov.br/. accessed 10.12.18).
Companhia de Pesquisa de Recursos Minerais - CPRM, 2012. Projeto avaliação do potential dos recursos minerais estratégicos do Brasil: área Carajás Oriental [WWW Document]. URL. http://geosgb.cprm.gov.br/. accessed 10.12.18).
Conselho Nacional de Meio Ambiente - Conama, 2012. Estabelece as diretrizes gerais e os procedimentos referenciais para o gerenciamento do material a ser dragado em águas sob jurisdição nacional. Correlações: Revoga as Resoluções Nº 344 de 2004 e Nº 421. Resolução CONAMA N° 454, de 01 de novembro de 2012. Diário Oficial da República Federativa do Brasil, Brazil.
Conselho Nacional de Meio Ambiente - Conama, 2009. Dispõe sobre critérios e valores orientadores de qualidade do solo quanto à presença de substâncias químicas e estabelece diretrizes para o gerenciamento ambiental de áreas contaminadas por essas substâncias em decorrência de atividades antrópicas. Resolução CONAMA N° 420. Diário Oficial da República Federativa do Brasil, Brazil de 28 de dezembro de 2009.
Conselho Nacional de Meio Ambiente - Conama, 2004. Estabelece as diretrizes gerais e os procedimentos mínimos para a avaliação do material a ser dragado em águas jurisdicionais brasileiras, e dá outras providências. Resolução CONAMA N° 344. Diário Oficial da República Federativa do Brasil, Brazil de 25 de março de 2004.
Costa, R. de V., Leite, M.G.P., Mendonça, F.P.C., Junior, H.A.N., 2015. Geochemical mapping of arsenic in surface waters and stream sediments of the Quadrilátero Ferrífero, Brazil. Geosciences 43–51. https://doi.org/10.1590/0370-44672015680077.
Costa, R. de V. da, Matschullat, J., Leite, M.G.P., Junior, H.A.N., Leão, L.P., 2018. Geochemical mapping of potentially hazardous elements in surface waters and stream sediments of the Quadrilátero Ferrífero. Brazil. Geochim. Bras. 32, 243–267. https://doi.org/10.21715/gb2358-2812.2018322243.
Dall'Agnol, R., Cunha, I.R.V. da, Guimarães, F.V., Oliveira, D.C. de, Teixeira, M.F.B., Feio, G.R.L., Lamarão, C.N., 2017. Mineralogy, geochemistry, and petrology of Neoarchean ferroan to magnesian granites of Carajás Province, Amazonian Craton: the origin of hydrated granites associated with charnockites. Lithos 277, 3–32. https://doi.org/10.1016/j.lithos.2016.09.032.
International geochemical mapping special issue. In: Darnley, A., Garrett, R.G. (Eds.), J. Geochem. Explor. 39.
Dall'Agnol, R., Oliveira, D.C., Guimarães, F.V., Gabriel, E.O., Feio, G.R.L., Lamarão, C.N., Althoff, F.J., Santos, P.A., Teixeira, M.F., Silva, A.C., Rodrigues, D.S., Santos, M.J.P., Silva, C.R.P., Santos, R.D., Santos, P.J.L., 2013. Geologia do subdomínio de transição do Domínio Carajás – implicações para a evolução arqueana da Província Carajás – Pará. 13 Simpósio de Geologia da Amazônia. SBG, Belém, pp. 1082–1085.
Darnley, A.G., Bjiirklund, A., Belviken, B., Gustavsson, N., Koval, P.V., Plant, J.A., Steenfelt, A., Tauchid, M., Xuejing, X., 1995. A Global Geochemical Database for Environmental and Resource Management : Recommendations for International Geochemical Mapping : Final Report of IGCP Project 259. UNESCO Publishing.
Deckere, E., De Cooman, W., Leloup, V., Meire, P., Schmitt, C., von der Ohe, P.C., 2011. Development of sediment quality guidelines for freshwater ecosystems. J. Soils Sediments 11, 504–517. https://doi.org/10.1007/s11368-010-0328-x.
Department of Environment, Conservation - DEC, 2010. Assessment levels for soil, sediment and water. Contaminated Sites Management Series, Version 4.
Doğan-Sağlamtimur, N., Kumbur, H., 2010. Metals (Hg, Pb, Cu, and Zn) bioaccumulation in sediment, fish, and human scalp hair: a case study from the city of mersin along the southern coast of Turkey. Biol. Trace Elem. Res. 136, 55–70. https://doi.org/10.1007/s12011-009-8516-5.
Environment Canada - EC, Ministere de l'Envionnement du Quebec - Menviq, 1992. Interim Criteria for Quality Assessment of St. Lawrence River Sediment. Environment Canada, Canada.
Epskamp, S., Costantini, G., Haslbeck, J., Cramer, A.O.J., Waldorp, L.J., Schmittmann, V. D., Borsboom, D., 2018. Graph Plotting Methods, Psychometric Data Visualization and Graphical Model Estimation.
Esri, 2016. ArcGIS for Desktop.
Feio, G.R.L., Dall'Agnol, R., 2012. Geochemistry and petrogenesis of the mesoarchean granites from the Canaã dos carajás area, carajás province, Brazil: implications for the origin of archean granites. Lithos 154, 33–52. https://doi.org/10.1016/j.lithos.2012.06.022.
Feio, G.R.L., Dall'Agnol, R., Dantas, E.L., Macambira, M.J.B., Santos, J.O.S., Althoff, F.J., Soares, J.E.B., 2013. Archean granitoid magmatism in the Canaã dos Carajás area: implications for crustal evolution of the Carajás province, Amazonian craton, Brazil. Precambrian Res. 227, 157–185. https://doi.org/10.1016/j.precamres.2012.04.007.
Fernandes, A.R., Souza, E.S., de Souza Braz, A.M., Birani, S.M., Alleoni, L.R.F., 2018. Quality reference values and background concentrations of potentially toxic elements in soils from the Eastern Amazon, Brazil. J. Geochem. Explor. 190, 453–463. https://doi.org/10.1016/j.gexplo.2018.04.012.
Filzmoser, P., 2015. StatDA: Statistical Analysis for Environmental Data.
Gallagher, V., Knights, K., Carey, S., Glennon, M., Scanlon, R., 2016. Atlas of stream sediment geochemistry of the northern counties of Ireland: data from the Tellus and Tellus Border projects. Geological Survey of Ireland.
Gałuszka, A., 2007. Different approaches in using and understanding the term "Geochemical background" - practical implications for environmental studies. Pol. J. Environ. Stud. 16, 389–395.
Gibbs, A.K., Wirth, K.R., Hirata, K.H., Olszewski Junior, W.J., 1986. Age and composition of the Grão Pará Group volcanics, Serra dos Carajás. Brazil. Rev. Bras. Geociencias 16, 201–211.
Grainger, C.J., Groves, D.I., Tallarico, F.H.B., Fletcher, I.R., 2008. Metallogenesis of the Carajás Mineral Province, southern Amazon Craton, Brazil: varying styles of archean through Paleoproterozoic to Neoproterozoic base- and precious-metal mineralisation. Ore Geol. Rev. 33, 451–489. https://doi.org/10.1016/j.oregeorev.2006.10.010.
Gross, J., Ligges, U., 2015. Nortest: Tests for Normality.
Hawkes, H.E., Webb, J.S., 1962. Geochemistry in Mineral Exploration. Harper & Row, New York.
Hin, J.A., Osté, L.A., Schmidt, C.A., 2010. Guidance Document for Sediment Assessment. Minist. Infrastruct. Environ. - DG Water.
Johnson, C.C., Ander, E.L., Cave, M.R., Palumbo-Roe, B., 2012. Normal background concentrations (NBCs) of contaminants in English soils: final project report. Br. Geol. Surv. Comm. Rep. CR/ 12/035, 40.
Kabata-Pendias, A., Pendias, H., 2001. Trace Elements in Soils and Plants, third ed. CRC Press, Boca Raton. https://doi.org/10.1201/b10158-25.
Labuschagne, L., Holdsworth, R., Stone, T., 1993. Regional stream sediment geochemical survey of South Africa. J. Geochem. Explor. 47, 283–296.
Larizzati, J.H., Marques, E.D., Silveira, F.V., 2014. Mapeamento geoquímico do Quadrilátero Ferrífero e seu entorno. Rio de Janeiro.
Larizzatti, J.H., Marques, E., Silveira, F., 2018. Geochemical mapping of Iron Quadrangle region by active stream sediments, state of Minas Gerais. Brazil. Geochim. Bras. 32, 268–292. https://doi.org/10.21715/gb2358-2812.2018322268.
Lima, A., De Vivo, B., Cicchella, D., Cortini, M., Albanese, S., 2003. Multifractal IDW interpolation and fractal filtering method in environmental studies: an application on regional stream sediments of (Italy), Campania region. Appl. Geochem. 18, 1853–1865. https://doi.org/10.1016/S0883-2927(03)00083-0.
Long, E., MacDonald, D., Smith, S., Calder, E., 1995. Incidence of adverse biological effects within ranges of chemical concentrations in marine and estuarine sediments. Environ. Manag. 19, 81–97.
Long, E.R., Morgan, L.G., 1990. The Potential for Biological Effects of Sediment-Sorbed Contaminants Tested in the National Status and Trends Program. National Oceanic and Atmospheric Admininistration, Seattle.
Macambira, M.J.B., Vasquez, M.L., Silva, D.C.C. da, Galarza, M.A., Barros, C.E. de M., Camelo, J. de F., 2009. Crustal growth of the central-eastern Paleoproterozoic domain, SW Amazonian craton: juvenile accretion vs. reworking. J. South Am. Earth Sci. 27, 235–246. https://doi.org/10.1016/j.jsames.2009.02.001.
MacDonald, D.D., Ingersoll, C.G., Berger, T.A., 2000. Development and evaluation of consensus-based sediment quality guidelines for freshwater ecosystems. Arch. Environ. Contam. Toxicol. 39, 20–31. https://doi.org/10.1007/s002440010075.
Machado, N., Lindenmayer, Z.G., Krogh, T.E., Lindenmayer, D., 1991. U-Pb geochronology of Archaean magmatism and basement reactivation in the Carajás area, Amazon shield, Brazil. Precambrian Res. 49, 329–354. https://doi.org/10.1016/0301-9268(91)90040-H.
Mansur, E.T., Ferreira Filho, C.F., 2017. Chromitites from the Luanga Complex, Carajás, Brazil: stratigraphic distribution and clues to processes leading to post-magmatic alteration. Ore Geol. Rev. 90, 110–130. https://doi.org/10.1016/j.oregeorev.2017.03.016.
Marangoanha, B., Oliveira, D.C. de, Oliveira, V.E.S. de, Galarza, M.A., Lamarão, C.N., 2019. Neoarchean A-type granitoids from Carajás province (Brazil): New insights from geochemistry, geochronology and microstructural analysis. Precambrian Res. 324, 86–108. https://doi.org/10.1016/j.precamres.2019.01.010.
Martins, P.L.G., Toledo, C.L.B., Silva, A.M., Chemale, F., Santos, J.O.S., Assis, L.M., 2017. Neoarchean magmatism in the southeastern Amazonian Craton, Brazil: petrography, geochemistry and tectonic significance of basalts from the Carajás Basin. Precambrian Res. 302, 340–357. https://doi.org/10.1016/j.precamres.2017.10.013.

Matschullat, J., Ottenstein, R., Reimann, C., 2000. Geochemical background–can we calculate it? Environ. Geol. 39, 990–1000.
Melo, G.H.C., Monteiro, L.V.S., Xavier, R.P., Moreto, C.P.N., Santiago, E.S.B., Dufrane, A., Aires, B., Santos, A.F.F., 2016. Temporal evolution of the giant Salobo IOCG deposit, Carajás Province (Brazil): constraints from paragenesis of hydrothermal alteration and U-Pb geochronology. Min. Depos. 52, 709–732.
Melo, V.F., Schaefer, C.E.G.R., Novais, R.F., Singh, B., Fontes, M.P.F., 2007. Potassium and magnesium in clay minerals of some Brazilian soils as indicated by A sequential extraction procedure. Commun. Soil Sci. Plant Anal. 33, 2203–2225. https://doi.org/10.1081/CSS-120005757.
Mineropar, 2001. Atlas geoquímico da folha Curitiba (SG-22-XD-I): sedimentos de fundo. Minerais do Paraná S. A. - MINEROPAR, Curitiba.
Ministry of the Environment of Finland - MEF, 2007. Government Decree on the Assessment of Soil Contamination and Remediation Needs, 214/2007 (March 1, 2007) [WWW Document]. URL. http://www.finlex.fi/en/laki/kaannokset/2007/en20070214.
Monteiro, L.V.S., Xavier, R.P., Hitzman, M.W., Juliani, C., de Souza Filho, C.R., Carvalho, E. de R., 2008. Mineral Chemistry of Ore and Hydrothermal Alteration at the Sossego Iron Oxide-Copper-Gold Deposit, Carajás Mineral Province, Brazil, Ore Geology Reviews. https://doi.org/10.1016/j.oregeorev.2008.01.003.
Moreto, C.P.N., Monteiro, L.V.S., Xavier, R.P., Creaser, R.A., DuFrane, S.A., Melo, G.H.C., Delinardo da Silva, M.A., Tassinari, C.C.G., Sato, K., 2014. Timing of multiple hydrothermal events in the iron oxide–copper–gold deposits of the Southern Copper Belt, Carajás Province, Brazil. Miner. Depos. 50, 517–546. https://doi.org/10.1007/s00126-014-0549-9.
Moreto, C.P.N., Monteiro, L.V.S., Xavier, R.P., Creaser, R.A., DuFrane, S.A., Tassinari, C. C.G., Sato, K., Kemp, A.I.S., Amaral, W.S., 2015. Neoarchean and Paleoproterozoic iron oxide-copper-gold events at the Sossego deposit, Carajás Province, Brazil: Re-Os and U-Pb geochronological evidence. Econ. Geol. 110, 809–835. https://doi.org/10.2113/econgeo.110.3.809.
Moura, C.A.V., Pinheiro, B.L.S., Nogueira, A.C.R., Gorayeb, P.S.S., Galarza, M.A., 2008. Sedimentary provenance and palaeoenvironment of the Baixo Araguaia Supergroup: constraints on the palaeogeographical evolution of the Araguaia belt and assembly of West Gondwana. Geol. Soc. London, Spec. Publ. 294, 173–196. https://doi.org/10.1144/sp294.10.
Paixão, M., Gorayeb, P.S. de S., 2014. Metalogênese da Faixa Araguaia. In: Silva, M. da G. (Ed.), Metalogênese Das Províncias Tectônicas Brasileiras. Serviço Geológico Do Brasil (CPRM), Brasília, p. 25.
Persaud, D., Jaagumagi, R., Hayton, A., 1993. Guidelines for the Protection and Management of Aquatic Sediment Quality in Ontario. Water Resources Branch. Ontario Ministry of the Environment, Toronto. https://doi.org/10.1080/00431672.1993.9930274.
Plant, J., Smith, D., Smith, B., Williams, L., 2001. Environmental geochemistry at the global scale. Appl. Geochem. 16, 1291–1308. https://doi.org/10.1016/S0883-2927(01)00036-1.
QGIS Development Team, 2009. QGIS Geographic Information System.
R Core Team, 2013. R: A Language and Environment for Statistical Computing.
Reimann, C., Caritat, P., 2017. Establishing geochemical background variation and threshold values for 59 elements in Australian surface soil. Sci. Total Environ. 578, 633–648. https://doi.org/10.1016/j.scitotenv.2016.11.010.
Reimann, C., Caritat, P., 2005. Distinguishing between natural and anthropogenic sources for elements in the environment: regional geochemical surveys versus enrichment factors. Sci. Total Environ. 337, 91–107. https://doi.org/10.1016/j.scitotenv.2004.06.011.
Reimann, C., Fabian, K., Birke, M., Filzmoser, P., Demetriades, A., Négrel, P., Oorts, K., Matschullat, J., de Caritat, P., Albanese, S., Anderson, M., Baritz, R., Batista, M.J., Bel-Ian, A., Cicchella, D., De Vivo, B., De Vos, W., Dinelli, E., Ďuriš, M., Duszа-Dobek, A., Eggen, O.A., Eklund, M., Ernsten, V., Flight, D.M.A., Forrester, S., Fügedi, U., Gilucis, A., Gosar, M., Gregorauskiene, V., De Groot, W., Gulan, A., Halamić, J., Haslinger, E., Hayoz, P., Hoogewerff, J., Hrvatovic, H., Husnjak, S., Jähne-Klingberg, F., Janik, L., Jordan, G., Kaminari, M., Kirby, J., Klos, V., Kwećko, P., Kuti, L., Ladenberger, A., Lima, A., Locutura, J., Lucivjansky, P., Mann, A., Mackovych, D., McLaughlin, M., Malyuk, B.I., Maquil, R., Meuli, R.G., Mol, G., O'Connor, P., Ottesen, R.T., Pasnieczna, A., Petersell, V., Pfleiderer, S., Poňavič, M., Prazeres, C., Radusinović, S., Rauch, U., Salpeteur, I., Scanlon, R., Schedl, A., Scheib, A., Schoeters, I., Šefčik, P., Sellersjö, E., Slaninka, I., Soriano-Disla, J.M., Šorša, A., Svrkota, R., Stafilov, T., Tarvainen, T., Tendavilov, V., Valera, P., Verougstraete, V., Vidojević, D., Zissimos, A., Zomeni, Z., Sadeghi, M., 2018. GEMAS: establishing geochemical background and threshold for 53 chemical elements in European agricultural soil. Appl. Geochem. 88, 302–318. https://doi.org/10.1016/j.apgeochem.2017.01.021.
Reimann, C., Filzmoser, P., Garrett, R.G., 2005. Background and threshold: critical comparison of methods of determination. Sci. Total Environ. 346, 1–16. https://doi.org/10.1016/j.scitotenv.2004.11.023.
Reimann, C., Filzmoser, P., Garrett, R.G., Dutter, R., 2008. Statistical Data Analysis Explained: Applied Environmental Statistics with R. John Wiley & Sons, Chichester.
Reimann, C., Garrett, R.G., 2005. Geochemical background - concept and reality. Sci. Total Environ. 350, 12–27. https://doi.org/10.1016/j.scitotenv.2005.01.047.
Ripin, S.N.M., Hasan, S., Kamal, M., 2014. Environmental geochemical mapping on distribution of metal contamination in topsoils perlis, Malaysia. J. Med. Bioeng. 3, 277–281. https://doi.org/10.12720/jomb.3.4.277-281.
Rodrigues, A.S. de L., Malafaia, G., Costa, A.T., Nalini Júnior, H.A., 2013. Background values for chemical elements in sediments of the Gualaxo do Norte River Basin, MG. Brazil. Rev. Ciências Ambient. 7, 18.
Rosa, W.D., 2014. Complexos acamadados da Serra da Onça e Serra do Puma: geologia e petrologia de duas intrusões máfico-ultramáficas com sequência de cristalização distinta na província arqueana de Carajás. Universidade de Brasília, Brasil.
RStudio Team, 2015. RStudio. Integrated Development for R.
Sahoo, P.K., Dall'Agnol, R., Salomão, G.N., da Silva Ferreira Junior, J., da Silva, M.S., Martins, G.C., e Souza Filho, P.W.M., Powell, M.A., Maurity, C.W., Angelica, R.S., da Costa, M.F., Siqueira, J.O., 2019a. Source and background threshold values of potentially toxic elements in soils by multivariate statistics and GIS-based mapping: a high density sampling survey in the Parauapebas basin, Brazilian Amazon. Environ. Geochem. Health. https://doi.org/10.1007/s10653-019-00345-z.
Sahoo, P.K., Dall'Agnol, R., Salomão, G.N., da Silva Ferreira Junior, J., Silva, M.S., e Souza Filho, P.W.M., Powell, M.A., Angélica, R.S., Pontes, P.R., da Costa, M.F., Siqueira, J.O., 2019b. High resolution hydrogeochemical survey and estimation of baseline concentrations of trace elements in surface water of the Itacaiúnas River Basin, southeastern Amazonia: implication for environmental studies. J. Geochem. Explor. https://doi.org/10.1016/j.gexplo.2019.06.003.
Salgado, S.S., Caxito, F.A., Queiroga, G.N., Castro, M.P., 2019. Stratigraphy, petrography and tectonics of the manganese-bearing Buritirama Formation, Northern Carajás Domain, Amazon Craton. Brazilian J. Geol. 49 https://doi.org/10.1590/2317-4889201920180106.
Salminen, R., Plant, J., Reeder, S., 2006. Geochemical Atlas of Europe: Background Information, Methodology and Maps. Geological Survey of Finland, Espoo.
Salminen, R., Tarvainen, T., 1997. The problem of defining geochemical baselines. A case study of selected elements and geological materials in Finland. J. Geochem. Explor. 60, 91–98. https://doi.org/10.1016/S0375-6742(97)00028-9.
Salminen, R., Tarvainen, T., Demetriades, A., Duris, M., Fordyce, F.M., Gregorauskiene, V., Kahelin, H., Kivisilla, J., Klaver, G., Klein, H., Larson, J.O., Lis, J., Locutura, J., Marsina, K., Mjartanova, H., Mouvet, C., O'Connor, P., Odor, L., Ottonello, G., Paukola, T., Plant, J.A., Reimann, C., Schermann, O., Siewers, U., Steenfelt, A., Van Der Sluys, J., DeVivo, B., Williams, L., 1998. FOREGS Geochemical Mapping, Field Manual. Geological Survey of Finland, Espoo.
Salomão, G., Dall'Agnol, R., Sahoo, P., Ferreira-Júnior, J., Silva, M., Souza-Filho, P., Berrêdo, J.F., Nascimento-Junior, W., Costa, M., 2018. Geochemical distribution and threshold values determination of heavy metals in stream water in the sub-basins of Vermelho and Sororó rivers, Itacaiúnas River watershed, Eastern Amazon, Brazil. Geochim. Bras. 32, 180–198. https://doi.org/10.21715/GB2358-2812.2018322180.
Salomão, G.N., Dall'Agnol, R., Angélica, R.S., Figueiredo, M.A., Sahoo, P.K., de Medeiros Filho, C.A., da Costa, M.F., 2019a. Geochemical mapping and estimation of background concentrations in soils of Carajás mineral province, eastern Amazonian Craton, Brazil. Geochem. Explor. Environ. Anal. 20 https://doi.org/10.1144/geochem2018-066 geochem2018-g2066.
Salomão, G.N., Figueiredo, M.A., Dall'Agnol, R., Sahoo, P.K., Medeiros Filho, C., Costa, M.F. da, Angélica, R., 2019b. Geochemical mapping and background determination of iron and potentially toxic elements in active stream sediments from Carajás, Brazil – implication for risk assessment. J. South Am. Earth Sci. 92 https://doi.org/10.1016/j.jsames.2019.03.014.
Santos, J.O.S., 2003. Geotectônica dos escudos das Guianas e Brasil-Central. In: Bizzi, L. A., Schobbenhaus, C., Vidotti, R.M., Gonçalves, J.H. (Eds.), Geologia, Tectônica e Recursos Minerais Do Brasil. Serviço Geológico do Braisl (CPRM), Brasília, pp. 169–195.
Santos, P.A., Feio, G.R.L., Dall'Agnol, R., Costi, H.T., Lamarão, C.N., Galarza, M.A., 2013. Petrography, magnetic susceptibility and geochemistry of the Rio branco granite, Carajás Province, Southeast of Pará, Brazil. Brazilian J. Geol. 43, 2–15. https://doi.org/10.5327/Z2317-48892013000100002.
Santos, J.O.S., Hartmann, L.A., Gaudette, H.E., Groves, D.I., Mcnaughton, N.J., Fletcher, I.R., 2000. A New understanding of the provinces of the Amazon craton based on integration of field mapping and U-Pb and Sm-Nd geochronology. Gondwana Res. 3, 453–488. https://doi.org/10.1016/S1342-937X(05)70755-3.
Sardinha, A.S., Barros, C.E. de M., Krymsky, R., 2006. Geology, geochemistry, and U-Pb geochronology of the Archean (2.74 Ga) Serra do Rabo Granite stocks, Carajás Metallogenetic Province, Northern Brazil. J. South Am. Earth Sci. 20, 327–339. https://doi.org/10.1016/j.jsames.2005.11.001.
Smith, S.L., MacDonald, D.D., Keenleyside, K.A., Ingersoll, C.G., Field, L.J., 1996. A preliminary evaluation of sediment quality assessment values for freshwater ecosystems. J. Great Lake. Res. 22, 624–638. https://doi.org/10.1016/S0380-1330(96)70985-1.
Soares, A., Mozeto, A.A., 2006. Water quality in the tietê river reservoirs (billings, barra bonita, bariri and promissão, SP-Brazil) and nutrient fluxes across the sediment-water interface (barra bonita). Acta Limnol. Bras. 18, 247–266.
Sousa, S.D. de, Monteiro, L.V.S., Oliveira, D.C. de, Delinardo da Silva, M.A., Moreto, C.P. N., Juliani, C., 2015. O Greenstone Belt Sapucaia na região de Água Azul do Norte, Província Carajás: contexto geológico e caracterização petrográfica e geoquímica. Contrib. a Geol. da Amaz. 9, 317–338.
Souza-Filho, P.W.M., Souza, E.B., Silva Júnior, R.O., Nascimento Jr., W.R., Mendonça, B. R.V., Guimarães, J.T.F., Dall'Agnol, R., Siqueira, J.O., 2016. Four decades of land-cover, land-use and hydroclimatology changes in the Itacaiúnas River watershed, southeastern Amazon. J. Environ. Manag. 167, 175–184. https://doi.org/10.1016/j.jenvman.2015.11.039.
Teng, Y., Ni, S., Wang, J., Niu, L., 2009. Geochemical baseline of trace elements in the sediment in Dexing area, South China. Environ. Geol. 57, 1649–1660. https://doi.org/10.1007/s00254-008-1446-2.
Tukey, J.W., 1977. Exploratory Data Analysis, first ed. Addison-Wesley Publishing Company, Massachusetts.
Ure, A.M., Berrow, M.L., 1982. The chemical constituents of soils. In: Bowen, H.J.M. (Ed.), Environmental Chemistry. Burlington House, London, pp. 94–102.

Vasquez, M.L., Sousa, C.S., Carvalho, K.M.A., 2008. Geologia e recursos minerais do estado do Pará. Belém.

Villas, R.N., Lima, A.D.P. de, Kotschoubey, B., Neves, M.P., Osborne, G.A., 2007. Contexto geológico e origem da mineralização sulfetada estratiforme de São Martim, SW do Cinturão Araguaia. Pará. Rev. Bras. Geociências 37, 305–323. https://doi.org/10.25249/0375-7536.2007373305323.

Wedepohl, K.H., 1978. Handbook of Geochemistry. Springer Verlag, Berlin. https://doi.org/10.1002/jobm.19800200529.

Xavier, R.P., Monteiro, L.V.S., Moreto, C.P.N., Pestilho, A.L.S., Melo, G.H.C. de, Silva, M.A.D., Aires, B., Ribeiro, C., Silva, F.H.F. e, 2012. The iron oxide copper-gold systems of the Carajás Mineral Province, Brazil. Special Publication 16. Society of Economic Geologists, pp. 433–454.

Yuan, G.L., Sun, T.H., Han, P., Li, J., 2013. Environmental geochemical mapping and multivariate geostatistical analysis of heavy metals in topsoils of a closed steel smelter: capital Iron & Steel Factory, Beijing, China. J. Geochem. Explor. 130, 15–21. https://doi.org/10.1016/j.gexplo.2013.02.010.

Zheng, Y., Sun, X., Gao, S., Wang, C., Zhao, Z., Wu, S., Li, J., Wu, X., 2014. Analysis of stream sediment data for exploring the Zhunuo porphyry Cu deposit, southern Tibet. J. Geochem. Explor. 143, 19–30. https://doi.org/10.1016/j.gexplo.2014.02.012.